



This discussion paper is/has been under review for the journal Hydrology and Earth System Sciences (HESS). Please refer to the corresponding final paper in HESS if available.

Integrated water system simulation by considering hydrological and biogeochemical processes: model development, parameter sensitivity and autocalibration

Y. Y. Zhang¹, Q. X. Shao², A. Z. Ye³, H. T. Xing^{1,4}, and J. Xia¹

¹Key Laboratory of Water Cycle and Related Land Surface Processes, Institute of Geographic Sciences and Natural Resources Research, Chinese Academy of Sciences, Beijing, 100101, China

²CSIRO Digital Productivity Flagship, Leeuwin Centre, 65 Brockway Road, Floreat Park, WA 6014, Australia

³College of Global Change and Earth System Science, Beijing Normal University, 100875, Beijing, China

⁴CSIRO Agriculture Flagship, GPO BOX 1666, Canberra, ACT 2601, Australia

Title Page

Abstract

Introduction

Conclusions

References

Tables

Figures



Back

Close

Full Screen / Esc

Printer-friendly Version

Interactive Discussion



Received: 1 April 2015 – Accepted: 29 April 2015 – Published: 22 May 2015

Correspondence to: Y. Y. Zhang (zhangyy003@igsnr.ac.cn)

Published by Copernicus Publications on behalf of the European Geosciences Union.

HESSD

12, 4997–5053, 2015

Integrated water system simulation

Y. Y. Zhang et al.

Title Page

Abstract

Introduction

Conclusions

References

Tables

Figures



Back

Close

Full Screen / Esc

Printer-friendly Version

Interactive Discussion



Abstract

Integrated water system modeling is a reasonable approach to provide scientific understanding of severe water crisis faced all over the world and to promote the implementation of integrated river basin management. Time Variant Gain Model (TVGM), which is a classic hydrological model, is based on the complex Volterra nonlinear formulation and has gotten good performance of runoff simulation in numerous basins. However, TVGM is disadvantageous to predict other water-related components. In this study, TVGM was extended to an integrated water system model by coupling multiple water-related processes in hydrology, biogeochemistry, water quality and ecology, and considering the interference of human activities. The parameter sensitivity and autocorrelation modules were also developed to improve the simulation efficiency. The Shaying River Catchment, which is the largest, highly regulated and heavily polluted tributary in the Huai River Basin of China, was selected as the study area. The key water related components (e.g., runoff, water quality, nonpoint source pollutant load and crop yield) were simulated. The results showed that the extended model produced good simulation performance of most components. The simulated daily runoff series at most regulated and less-regulated stations matched well with the observations. The average values of correlation coefficient and coefficient of efficiency between the simulated and observed runoffs were 0.85 and 0.70, respectively. The simulations of both low and high flow events were improved when the dam regulation was considered except the low flow simulation at Zhoukou and Huaidian stations. The daily ammonia-nitrogen ($\text{NH}_4\text{-N}$) concentration, as a key index to assess water quality in China, was well captured with the average correlation coefficient of 0.67. Furthermore, the nonpoint source $\text{NH}_4\text{-N}$ load and corn yield were simulated for each administrative region and the results were reasonable in comparison with the data from the official report and the statistical yearbooks, respectively. This study is expected to provide a scientific support for the implementation of such a modeling practice for integrated river basin management.

Integrated water system simulation

Y. Y. Zhang et al.

Title Page

Abstract

Introduction

Conclusions

References

Tables

Figures



Back

Close

Full Screen / Esc

Printer-friendly Version

Interactive Discussion



1 Introduction

Severe water crises are global issues emerged in the rapid development of social economy, including flooding (Milly et al., 2002; Schiermeier et al., 2011), water shortages (Pimentel et al., 2004; Wilhite et al., 2005), water pollution (Jordan et al., 2014; Zhou et al., 2014) and ecological degradation (Revenga et al., 2000; Vörösmarty et al., 2010). These issues are hindering regional equitable development by compromising the sustainability of vital water resource and ecosystem (Gleick, 1997). It is impossible to address these water-related problems within a single scientific discipline (e.g., hydrology, hydraulics, water quality or aquatic ecology) due to the complicated interconnections among the physical, chemical and ecological components of an aquatic ecosystem (Kindler, 2000; Biswas, 2004; Paola et al., 2006). The integrated river basin management might be a sensible solution at basin scale by the coordinated management of water resources among the social-economy, water quality and ecosystems (Rahaman and Varis, 2005; Hering et al., 2012). Integrated water system modeling is a reasonable practice to simultaneously simulate water related components (flow regimes, nutrient loss, sediment and water pollution), and also an effective tool to support water resource allocation, environmental flow management and river restoration (Arthington, 2012).

Integrated water system modeling has gained popularity due to the rapid development of water related sciences, computer sciences and earth observation technologies in the last decades. The hydrological cycle has been widely accepted as a critical linkage among physical (e.g., runoff), biogeochemical (e.g., nutrient, water quality) and ecological processes (e.g., plant growth), energy fluxes at basin scale (Wigmosta et al., 1994; Singh and Woolhiser, 2002; Burt and Pinay, 2005). For example, the physiological and ecological processes of vegetation affect evapotranspiration, soil moisture distribution and infiltration, and nutrients absorption and movement. On the contrary, soil moisture and nutrient content directly affect crop growth. Overland flow is a carrier of the pollutant load discharge to water body (Li et al., 1992; Lohse et al., 2009). Therefore, it is reasonable to analyze variation patterns of water related components and their

HESSD

12, 4997–5053, 2015

Integrated water system simulation

Y. Y. Zhang et al.

Title Page

Abstract

Introduction

Conclusions

References

Tables

Figures

⏪

⏩

◀

▶

Back

Close

Full Screen / Esc

Printer-friendly Version

Interactive Discussion



HESSD

12, 4997–5053, 2015

Integrated water system simulation

Y. Y. Zhang et al.

[Title Page](#)[Abstract](#)[Introduction](#)[Conclusions](#)[References](#)[Tables](#)[Figures](#)[|◀](#)[▶|](#)[◀](#)[▶](#)[Back](#)[Close](#)[Full Screen / Esc](#)[Printer-friendly Version](#)[Interactive Discussion](#)

causes at the basin scale by coupling all these processes and capturing the interactions and feedbacks between individual cycles. Furthermore, multidisciplinary research provides an effective way to make possible breakthroughs in water system modeling by integrating the mature basic theories of water-related disciplines (e.g., accumulated temperature law for phenological development, Darcy's law for groundwater flow, Saint-Venant Equation for surface flow, balance equation for mass and momentum, Richards equation for unsaturated zone, Horton theory for infiltration, Penman–Monteith equation for evapotranspiration), and abundant data sources (e.g., high resolution of spatial information data: DEM, land use and crop distribution, chemical and isotopic data from field experiment) (Singh and Woolhiser, 2002; Kirchner, 2006).

Several models have been developed based on the mature models of different disciplines since the 1980s (Singh and Woolhiser, 2002). Due to the complexity of the integrated system, most of existing models focus on one or two major water related processes, depending on the model orientation (e.g., hydrology, water quality, and biogeochemistry). The hydrological models emphasize on the rainfall–runoff relationship and link with several dominating water quality and biogeochemical processes. As a result, these models usually have satisfactory performance in major hydrological processes. Examples of widely accepted models include TOPMODEL (Beven and Kirkby, 1979), SHE (Abbott et al., 1986), HSPF (Bicknell et al., 1993), VIC (Liang et al., 1994) and ANSWERS (Bouraoui and Dillaha, 1996). The water quality models focus on the migration and transformation processes of pollutants in water bodies. The models can get the detailed spatial and temporal variations of water quality variables in river system by adopting multi-dimensional dynamic equation, but are difficult to simulate the overland processes of water and pollutants. The typical models are WASP (Di Toro et al., 1983), QUAL2E (Brown and Barnwell, 1987), EFDC (Hamrick, 1992). The biogeochemistry models have advantages to simulate physiological and ecological processes of vegetation, vertical movement of nutrients and water in soil layers at the field or experimental catchment scales, but lack the accurate hydrological features (Deng et al., 2011). Thus it is hard to simulate the movement of water, nutrients and their losses along flow path-

ways in the basin. The examples are EPIC (Sharpley and Williams, 1990), DND (Li et al., 1992).

SWAT is a typical integrated water system model, which simulates most of water related processes over long time periods at large scales and has been widely accepted (Arnold et al., 1998). Its model structure and functions are considered as a landmark in the field of water system modeling. However, not all of water related processes could be well captured in practice due to the applicability and inaccurate descriptions of some modules, such as daily simulations of extreme flow events (Borah and Bera, 2004), soil nitrogen and carbon (Gassman et al., 2007), the performance in regulated basins (Zhang et al., 2012). Particularly, SWAT applies two alternative approaches to simulate surface runoff, e.g., the empirical Soil Conservation Service (SCS) curve number method and the conceptual Green–Ampt infiltration model. The SCS equation is usually given priority, but the applicability of curve number is questioned (Rallison and Miller, 1981). The Green–Ampt infiltration model is usually limited to simulate flow events at micro temporal and spatial scales (Brakensiek, 1977; King et al., 1999). Furthermore, it is much more difficult for SWAT to capture the complicated dynamic processes of soil nitrogen and carbon accurately in comparison with other biochemistry models (Gassman et al., 2007). Polhert et al. (2006, 2007) was extended SWAT with algorithms from DND (SWAT-N), and found that SWAT-N could be used for monthly and weekly prediction of nitrate load, but should be avoided for daily prediction.

Time Variant Gain Model (TVGM) is a lumped hydrological model, which was proposed by Xia (1991) based on the hydrological data from many different scales basins all over the world. In TVGM, the rainfall–runoff relationship is considered to be nonlinear with surface runoff coefficient varying over time and being affected significantly by antecedent soil moisture (Xia et al., 1991). TVGM has strong mathematics basis because this nonlinear relationship can be transformed into the complex Volterra nonlinear formulation. Wang et al. (2002) extended TVGM to the distributed model (DTVGM) due to better computing facilities and available data sources. Currently, DTVGM was widely used in many basins of different scales and in different climate zones to investigate

HESSD

12, 4997–5053, 2015

Integrated water system simulation

Y. Y. Zhang et al.

Title Page

Abstract

Introduction

Conclusions

References

Tables

Figures

⏪

⏩

◀

▶

Back

Close

Full Screen / Esc

Printer-friendly Version

Interactive Discussion



the impact of human activities and climate change on runoff, and got good simulation performance (Xia et al., 2005; Wang et al., 2009). However, DTVGM was confined to the studies of hydrological cycle and could not be applied to the integrated river basin management due to the lack of considering other water-related processes, such as the water quality processes, ecological processes, soil biogeochemical processes.

The objective of this study is to extend DTVGM to an integrated water system model by considering hydrological, biogeochemical, water quality and ecological processes, and the prevalent regulation by water projects, with the aim to meet the demand of the integrated river basin management. The model framework is developed based on the interchange among the processes of water and nutrient depicted by several robust models. The parameter analysis module is also included in our programming codes. The extended model is expected to capture the spatial and temporal variations of several key water-related components (e.g., flow regimes, nonpoint source pools of nutrients, water quality variables in water body and crop yield) in complex basins.

2 Methods and material

2.1 Model framework

The proposed model includes seven major modules, named as hydrological cycle module (HCM), soil biochemical module (SBM), crop growth module (CGM), soil erosion module (SEM), overland water quality module (OQM), water quality module of water bodies (WQM) and dam regulation module (DRM). Parameter analysis tool (PAT) is a useful tool for model calibration and is independent from other modules. The exterior exchange components connecting different modules are given in Fig. 1. More detailed description of each module and its interactions with other modules are given in the following individual Sects. from 2.1.1 to 2.1.6. The main equations of each process are deferred to the appendix and supplementary material section for readers who are interested in the mathematical details.

HESSD

12, 4997–5053, 2015

Integrated water system simulation

Y. Y. Zhang et al.

Title Page

Abstract

Introduction

Conclusions

References

Tables

Figures

⏪

⏩

⏴

⏵

Back

Close

Full Screen / Esc

Printer-friendly Version

Interactive Discussion



age routing methodology (Neitsch et al., 2011). The Muskingum method or kinetic wave equation is used for river flow routing.

A flowchart is given in Fig. 2, from which it can be seen that shallow soil water from the hydrological cycle module is one of the major factors connecting the crop growth module (to control crop growth) and the soil biochemical module (to control vertical migration and reaction of nutrients in the soil profiles). Plant transpiration is also linked to the soil biochemical module (to provide energy for vertical migration of nutrients in the soil profiles). The surface runoff is linked to the soil erosion and the overland flow is connected to the overland water quality modules (to drive migration of nutrients and sediment along flow paths) and water quality module for runoff routing in water bodies (rivers and lakes). Moreover, the hydrological cycle module calculates inflow of dam or sluice for the dam regulation module.

2.1.2 Ecological process modules

Ecosystem is one of the decisive components to the hydrological cycle and the pollutant migration and transportation. The model incorporates the water cycle, nutrient cycles and crops growth, as well as their key linkages. The ecological process modules contain SBM and CGM.

Soil biochemical module (SBM)

The soil biochemical module simulates the key processes of Carbon (C), Nitrogen (N) and Phosphorus (P) dynamics in the soil profiles, including decomposition, mineralization, immobilization, nitrification, denitrification, plant uptake and leaching. C constrains the decomposition and denitrification of N and P. Different forms of nutrients (N and P) outputted from the soil biochemical module are connected to the crop growth module as the nutrient constraints of crop growth, and to the overland water quality module as the main nonpoint sources of pollutant to water bodies (Fig. 3a). The daily step decomposition and denitrification submodels in DNDC are adopted to simulate bio-

HESSD

12, 4997–5053, 2015

Integrated water system simulation

Y. Y. Zhang et al.

Title Page

Abstract

Introduction

Conclusions

References

Tables

Figures

⏪

⏩

◀

▶

Back

Close

Full Screen / Esc

Printer-friendly Version

Interactive Discussion



Integrated water system simulation

Y. Y. Zhang et al.

Title Page

Abstract

Introduction

Conclusions

References

Tables

Figures

I◀

▶I

◀

▶

Back

Close

Full Screen / Esc

Printer-friendly Version

Interactive Discussion



geochemical processes of C and N in the soil profile at field scale, which is variable according to the crop pattern in the actual situation (Li et al., 1992). The major processes of soil P cycle are simulated based on the study of Horst et al. (2001). The soil profile is divided into three layers, e.g., surface (0–10 cm), and user defined upper and lower layer, all of which are consistent with the soil layers of hydrological cycle module in order to exchange the values of linkages (e.g., soil water) among different modules smoothly.

Soil C and N cycle. The decomposition and other oxidation processes are the dominant microbial processes in the aerobic condition, while the denitrification process occurs under anaerobic condition.

- *Decomposition.* There are three conceptual organic C pools: the decomposable residue pool, microbial biomass pool and a stable pool (humus). Every pool contains resistant and labile components. Additionally, the residue pool contains a very labile component. The decomposition of each C pool is treated as the first-order decay process with the individual decomposition being modified by soil temperature and moisture, clay content and the C : N ratio. Carbon dioxide (CO₂), released from soil organic carbon (SOC), is calculated as a constant fraction of the C undergoing decomposition of three C pools. When the soil water filled pore space (WFPS) in the surface soil layer is increased over 55 % by precipitation and/or irrigation, the decomposition process will pause and the denitrification process will start. The decomposition will start again and denitrification will stop when WFPS is below 55 % or the substrates are used up. The details of SOC pool structure are described in Li et al. (1992).
- *Nitrogen transformation during decomposition.* The major simulated processes of decomposition under aerobic condition are mineralization, immobilization, ammonia (NH₃) volatilization and nitrification. Ammonium (NH₄⁺) is mineralized from organic N pool when SOC flows from C pool with lower C : N ratio into C pool with higher C : N ratio or CO₂ is released into air during SOC decomposition. Mineral

Integrated water system simulation

Y. Y. Zhang et al.

Title Page

Abstract

Introduction

Conclusions

References

Tables

Figures

⏪

⏩

◀

▶

Back

Close

Full Screen / Esc

Printer-friendly Version

Interactive Discussion



N (NO_3^- and NH_4^+) is immobilized into soil organic N pool, when SOC flows from the higher C : N ratio C pools into the lower C : N ratio C pools. Model assumes that the flow rate of SOC from the higher C : N ratio C pool to the lower C pool (higher C : N ratio C pool decomposition) will reduce to an allowable level to meet the available mineral N if the mineral N is not enough. NH_3 volatilization is controlled by the simulated NH_4^+ concentration, clay content, pH, soil moisture and temperature. NH_4^+ is microbial oxidized to NO_3^- and nitrous oxide (N_2O) which emit into the air as a gaseous intermediate matter during nitrification. The proportion of N_2O is controlled by NH_4^+ concentration, pH, temperature, moisture in the soil layer.

– *Denitrification.* The denitrification process occurs when WFPS is greater than the threshold (55 %) during rainfall or irrigation events. The generally recognized reduction sequence in denitrification is $\text{NO}_3^- \rightarrow \text{NO}_2 \rightarrow \text{NO} \rightarrow \text{N}_2\text{O} \rightarrow \text{N}_2$. The denitrification rate correlates with denitrifier biomass, moisture, pH, temperature and NO_3^- concentration in the soil layer. The denitrifier biomass is estimated with the growth and dead rate of denitrifier which is controlled by dissolved soil organic C, soil moisture and temperature. The C and N from dead cells are added to the pools of immobilized C and N which no longer participate in the dynamic processes. The consumption rate of soluble C depends on the biomass, relative growth rate, and the maintenance coefficients of the denitrifier populations. The daily emission rates of greenhouse gases (N_2O , NO and N_2) are related to the adsorption coefficients of gases in soils and the air filled porosity of the soil. But N_2O and NO emissions are neglected because of the low diffusion rates in soil water if WFPS is over 90 %.

Soil P cycle. Six P pools are considered, e.g., three organic pools (stable and active pools for plant uptake, fresh pool associated with plant residue) and three mineral pools (soluble mineral, stable and active pools) as the consequence of mineralization, decomposition and sorption (Horst et al, 2001). The P dynamics processes are con-

sidered in Horst et al. (2001) and Neitsch et al. (2011), through modeling the P release from fertilizer, manure, residue, microbial biomass and humic substances, P sorption by plant uptake, and P transportation by sediment and overland flow.

Crop growth module (CGM)

5 The crop growth module is developed based on EPIC crop growth model (Hamrick, 1992), which applies the concept of daily accumulated heat units on phenological crop development, Monteith's approach for potential biomass, harvest index for partitioning grain yield, and stress adjustments for water, temperature and nutrient (N and P) availability in the root zone of the soil profile. It simulates total dry matter, leaf area index, 10 root depth and density distribution, harvest index, nutrient uptake, etc (Williams et al., 1989; Sharpley and Williams, 1990). The crop respiration and photosynthesis drive the vertical movement of water and nutrient. In the crop growth module, the output of leaf area index is the main factor connecting the hydrological cycle module (to control the transpiration), and the crop residue left in the fields is the main source of organic 15 matters (C, N and P) connecting to the soil biochemical module for soil biochemical processes, to the overland water quality module, and to the soil erosion module as one of the five constraint factors (Fig. 3b).

2.1.3 Water quality process modules

20 The water quality process modules focus on the migration and transformation of water quality variables (e.g., sediment, different forms of nutrients, chemical oxygen demand: COD) along with the water movement in the land surface and river systems. The main modules are the soil erosion module for the sediment yield, the overland water quality module for the nonpoint source pollutant loss and migration from the soil layers to water bodies (rivers or lakes), and the water quality module for the migration and 25 transformation of pollutants in the water bodies (point and non-point source loads).

Integrated water system simulation

Y. Y. Zhang et al.

Title Page

Abstract

Introduction

Conclusions

References

Tables

Figures

⏪

⏩

◀

▶

Back

Close

Full Screen / Esc

Printer-friendly Version

Interactive Discussion



Soil erosion module (SEM)

The soil erosion by precipitation is estimated using the improved USLE equation (Onstad and Foster, 1975) based on runoff outputted from the hydrological cycle module, crop management factor outputted from the crop growth module. The soil erosion module simulates sediment load for the overland water quality module to provide the carrier for the migration of insoluble organic matters along overland transport paths and water bodies (Fig. 4a).

Overland water quality module (OQM)

This module is to simulate the overland loss and migration load of nonpoint source pollutant (e.g., sediment, insoluble and soluble nutrients, COD) for the water quality module of water bodies (Fig. 4b). Their main sources are the nutrient loss from the soil layers and urban area, the farm manure from living and livestock breeding in the rural area. The nutrient loss from the soil layers, as the primary nonpoint source in most catchments, is determined by the overland flow and sediment yield (Williams et al., 1989; Neitsch et al., 2011) and the other sources are estimated using the export coefficient method (Johnes, 1996; Lin, 2004). The overland migration processes contain the soluble pollutant migration with overland flow and the insoluble pollutant migration with sediment. All of these processes take place along the overland transport paths.

Water quality module of water bodies (WQM)

There are point and nonpoint sources of pollutant discharged into water bodies in the basins. The point source load is the direct input of our proposed model, including the observed urban inhabitant and industrial sewage discharged into river network while the nonpoint source load is simulated by the overland water quality module.

Two modules are designed for different types of water bodies, e.g., the in-stream water quality module and the water quality module of water impounding (reservoir or lake).

HESSD

12, 4997–5053, 2015

Integrated water system simulation

Y. Y. Zhang et al.

Title Page

Abstract

Introduction

Conclusions

References

Tables

Figures

◀

▶

◀

▶

Back

Close

Full Screen / Esc

Printer-friendly Version

Interactive Discussion



Integrated water system simulation

Y. Y. Zhang et al.

Title Page

Abstract

Introduction

Conclusions

References

Tables

Figures

I◀

▶I

◀

▶

Back

Close

Full Screen / Esc

Printer-friendly Version

Interactive Discussion



The enhanced stream water quality model (QUAL-2E) (Brown and Barnwell, 1987), as a comprehensive and versatile stream model, is adopted to simulate the longitudinal movement and transformation of water quality variables in the branch stream systems. The model is centered at dissolved oxygen (DO) and can simulate up to 15 water quality variables including temperature, DO, sediment, different forms of nutrient (N and P), COD (Fig. 4c). The model is solved at the subbasin scale rather than the fine grid scale. The water quality outputs are linked to the dam regulation module to provide upper water quality boundary of dams or sluices. The water quality module of water impounding assumes that water body is at the steady state and focuses on the vertical interaction of water quality. The main processes are the water quality degradation, settlement, resuspension and decay in the sediment.

2.1.4 Dam regulation module (DRM)

The dams or sluices highly disturb flow regimes and associated water quality processes in most river networks (Zhang et al., 2013). The dam or sluice regulation should be considered in the water system models. The dam regulation module provides hydrological boundaries (e.g., water storage, runoff) regulated by dams or sluices to the hydrological cycle module for flow routing and to the water quality module of water bodies for pollutant migration.

In this module, three methods are proposed for calculating water storage and outflow of dams or sluices, i.e., measured outflow, controlled outflow with target water storage, and the relationship between outflow and water storage volume (Zhang et al., 2013). The first method requires users to provide the measured outflow series during the simulation period. The second method simplifies the regulation rule of dam or sluice for the long-term analysis by assuming that water is stored according to the usable water level during the non-flooding season and the flood control level during the flooding season and that the redundant water is discharged. This method requires the characteristic parameters of dam or sluice including water storage capacities of dead, usable, flood control and maximum flood levels and the corresponding water surface areas. The third

method is proposed based on relationship among water level, water surface area, storage volume and outflow according to the design data of dam, or long-term observed data (Appendix C).

2.1.5 Multi-scale solution

5 Spatial heterogeneities of basin attributes and inconsistent reaction times of different processes result in the multiple spatial and temporal scales of hydrological, water quality and ecological processes (Blöschl and Sivapalan, 1995; Sivapalan and Kalma, 1995; Singh and Woolhiser, 2002; Lohse et al., 2009). For the spatial scale, three levels of spatial calculation units are designed in the model, i.e. subbasin unit, landuse
10 unit and crop unit from largest to smallest. These units are the minimum polygons with similar hydrological properties, landuse type and agriculture crop cultivation pattern, respectively. The subbasins are defined on the basis of DEM, the position of gauges and water projects (dams or sluices), and are used in the hydrological cycle module (e.g., flow routing in both land and in-stream), overland water quality module, water
15 quality module of water bodies and dam regulation module. Seven specific landuse units of each subbasin are partitioned by the landuse classification (e.g., forest, grassland, water, urban, unused land, paddy land and dry land). The related modules are the hydrological cycle module (e.g., water yield, infiltration, interception and evapotranspiration) and soil erosion module. Moreover, several specific landuse units (paddy land
20 and dry land, forest, grassland), where agricultural activities usually occur, are divided further into crop units for detailed analysis of the impact of agricultural management on water and nutrient cycles. In the current version of the model, ten specific categories of crop units are divided for these four landuse units, i.e. fallow for all these landuse units; grass for grassland unit; fruit tree and non-economic tree for forest unit; early rice and late rice for paddy unit; spring wheat, winter wheat, corn, and mixed dry crop
25 for dry land unit. The crop unit category of a certain landuse is variable, depending on crop cultivation structure and timing. The related modules are the soil biochemical module and the crop growth module. All the outputs of crop unit are summarized at the

Integrated water system simulation

Y. Y. Zhang et al.

Title Page

Abstract

Introduction

Conclusions

References

Tables

Figures

⏪

⏩

◀

▶

Back

Close

Full Screen / Esc

Printer-friendly Version

Interactive Discussion



landuse unit scale, or subbasin scale based on the area percentage of different units, respectively.

For the temporal scale, the time step of our proposed model is one day because most simulated processes are usually considered to take place at daily scale (Lohse et al., 2009). The linear or nonlinear aggregating functions are used to transform different time scales to the daily scale (Vinogradov et al., 2011), such as exponential relation for the flow infiltration and overland flow routing processes, soil erosion processes (A5, A6 and S32), accumulative relation for the crop growth process (S7 in the Supplement).

2.1.6 Basic datasets and spatial delineation

The indispensable datasets of the proposed model are GIS data (DEM, soil physical and chemical properties, land use and crop types), daily meteorological data series (precipitation, maximum and minimum air temperature), social and economic data series (population and livestock number in rural area, chemical fertilizer types, amount and cultivation methods, water withdrawal and point source pollutant load), dam attribute data (water storage capacities of dead, usable, flood control and maximum flood levels and the corresponding water surface areas). Several monitoring data series are also needed for model calibration, such as runoff and water quality series at river sections, soil water moisture and crop yield at the field scale. All the datasets and their usages are given in Table 1.

The hydrological toolset of Arc GIS platform are used to delineate all the spatial calculation units and river system based on DEM, landuse data. The subbasin attributes (e.g., subbasin area, land surface slope and slope length) and flow routing relationship between subbasins are also obtained during this procedure.

2.2 Parameter analysis and calibration

Parameter sensitivity analysis and auto-calibration are critical steps for the applications of highly parameterized models and are treated more and more seriously, espe-

HESSD

12, 4997–5053, 2015

Integrated water system simulation

Y. Y. Zhang et al.

Title Page

Abstract

Introduction

Conclusions

References

Tables

Figures

⏪

⏩

◀

▶

Back

Close

Full Screen / Esc

Printer-friendly Version

Interactive Discussion



Integrated water system simulation

Y. Y. Zhang et al.

Title Page

Abstract

Introduction

Conclusions

References

Tables

Figures

◀

▶

◀

▶

Back

Close

Full Screen / Esc

Printer-friendly Version

Interactive Discussion



cially for the integrated water system models (Mantovan and Todini, 2006; Mantovan et al., 2007; McDonnell et al., 2007). In the model, nearly 200 parameters (78 lumped and 104 distributed) involve the hydrological, ecological and water quality processes. The distributed parameters are divided into 46 overland parameters, 18 stream parameters and 40 parameters of water projects (only for the subbasin having reservoir or sluice) according to their spatial distribution. These parameter values were determined by the properties of overland landscape and soil, stream patterns and water projects, respectively. Different spatial calculation units share many common parameter values if their properties were the same.

PAT is designed for parameter analysis, and is independent from the extended model (Fig. 5). Several parameter analysis methods are adopted, including parameter sensitivity method (Latin Hypercube One factor At a Time: LH-OAT) (van Griensven et al., 2006), auto-optimization methods such as Particle Swarm Optimization (PSO) (Kennedy, 2010), Genetic Algorithm (GA) (Goldberg, 1989) and Shuffled Complex Evolution (SCE-UA) (Duan et al., 1994). Five indices are provided to evaluate model performance including bias (bias), relative error (re), root mean square error (RMSE), correlation coefficient (r) and coefficient of efficiency (NS). These methods and indices were selected to use in the model application based on specific requirements by users.

2.3 Study area and model testing

In this study, the extended model was applied in a highly regulated and heavily polluted river basin of China in order to test the model performance. The simulated components contained daily runoff and water quality concentration at several river cross-sections, spatial patterns of nonpoint source pollutant load and crop yield at subbasin scale.

2.3.1 Study area

Shaying River Catchment ($112^{\circ}45' \sim 113^{\circ}15' \text{ E}$, $34^{\circ}20' \sim 34^{\circ}34' \text{ N}$), as the largest sub-basin of Huai River Basin in China, is selected as our study area (Fig. 6a). It has the

Integrated water system simulation

Y. Y. Zhang et al.

Title Page

Abstract

Introduction

Conclusions

References

Tables

Figures

◀

▶

◀

▶

Back

Close

Full Screen / Esc

Printer-friendly Version

Interactive Discussion



drainage area of 36 651 km² and the mainstream of 620 km. The average annual population (2003–2008) (Fig. 6b) is 32.42 million including 23.70 million rural population. The average annual stocks (Fig. 6c) are 8.30 million (big animals) and 178.42 million (poulties), respectively. The average annual use of chemical fertilizer (Fig. 6d) is 1.55 million ton (N: 38 ~ 51 %, P: 16 ~ 25 %, K: 7 ~ 12 % and others: 16 ~ 35 %). The basin is located in the typical warm temperate, semi-humid continental climate zone. The annual average temperature and rainfall are 14–16 °C and 769.5 mm, respectively. Meanwhile, Shaying River is the most serious polluted tributary with pollutant load contributing over 40 % of the whole Huai River and is usually known as the water environment barometer of Huai River mainstream. In order to reduce flood or drought disasters, 24 reservoirs and 13 sluices have been constructed and fragment river into several impounding pools which control over 50 % of the total annual runoff.

2.3.2 Model setup

The Shaying River Catchment was divided into 46 subbasins. According to the landuse classification standard of China (CNS, 2007), the main land use types were dry land (84.04 %), forest (7.66 %), urban (3.27 %), grassland (2.68 %), water (1.43 %), paddy (0.91 %) and unused land (0.01 %). The soil input parameters (the contents of sand, clay and organic matter) were calculated based on the percentage of soil types in each subbasin. The main crops were the early rice and late rice in the paddy land, and the winter wheat and corn in the dry land. Their main agricultural management schemes (fertilization, plant, harvest and kill) were summarized by field investigation referred to Wang et al., (2008) and Zhai et al. (2014) (Table 2). The crop rotation and their management schemes were considered in the model by setting the start time and duration of management and the fertilizer amounts used. Only two fertilizations (base and additional fertilization) were designed in the model during the complete growth cycle of a certain crop. The areas of subbasin, landuse and crop unit ranged from 46.48 to 3771.15 km², from 0.04 to 2762.5 km², and from 3.73 to 2762.5 km², respectively.

**Integrated water
system simulation**

Y. Y. Zhang et al.

[Title Page](#)[Abstract](#)[Introduction](#)[Conclusions](#)[References](#)[Tables](#)[Figures](#)[|◀](#)[▶|](#)[◀](#)[▶](#)[Back](#)[Close](#)[Full Screen / Esc](#)[Printer-friendly Version](#)[Interactive Discussion](#)

The daily data series at 65 precipitation stations and six temperature stations were interpolated to each subbasin from 2003 to 2008, using the inverse distance weighting method and the nearest-neighbor interpolation method, respectively. The social and economic data (e.g., population and livestock in the rural area, chemical fertilizer amount) were calculated for each subbasin based on the area percentage.

Moreover, 23 major dams and sluices and more than 200 urban wastewater discharge outlets were considered in the model according to the geographical positions. The farm manure from rural living and livestock farming were considered in the model as nonpoint source due to the scattered characteristics and the deficiency sewage treatment facilities in the rural area.

2.3.3 Model evaluation

$\text{NH}_4\text{-N}$ concentration is one of the widely used indices to assess water quality condition in China (CSEPA, 2002). Thus, both the observation series of daily runoff and $\text{NH}_4\text{-N}$ concentration were used to calibrate the model parameters. There were five regulated stations (Luohe, Zhoukou, Huaidian, Fuyang and Yingshang) and one unregulated station (Shenqiu) (e.g., the upstream stations unaffected by water projects, or downstream stations situated far from water projects).

We selected LH-OAT for parameter sensitivity analysis and SCE-UA for parameter calibration in the PAT. The initial parameter values were preset randomly from the value ranges determined by their physical characteristics. The evaluation indices used are bias, r and NS as a demonstration of the extended model. However, NS is sensitive to extreme value, outlier and number of data points and is not commonly applied in the environmental sciences (Ritter and Muñoz-Carpena, 2013). Thus NS was not used to evaluate the $\text{NH}_4\text{-N}$ concentration simulation. Furthermore, as the real observed yields of nonpoint pollutant loads and crops were hard to collect for the whole catchment (Chen et al., 2014), their simulations were only evaluated preliminarily using the bias according to the statistical results from the official report or the statistical yearbooks (Wang, 2011; Henan Statistical Yearbook, 2003, 2004 and 2005).

Title Page

Abstract

Introduction

Conclusions

References

Tables

Figures

I◀

▶I

◀

▶

Back

Close

Full Screen / Esc

Printer-friendly Version

Interactive Discussion



The model calibration was conducted step-by-step as follows. Hydrological parameters were calibrated first against the observed runoff series at each station from upstream to downstream, and then water quality parameters against the observed $\text{NH}_4\text{-N}$ concentration series. The calibration and validation periods were from 2003 to 2005 and from 2006 to 2008, respectively. To reduce the dimensions of the calibration problem, we restricted SCE-UA to calibrate only the sensitive parameters as defined by LH-OAT. Weighting method was usually used to comprehensively handle different objectives (Efstratiadis and Koutsoyiannis, 2010). In this study, these objective functions were simply aggregated to single objectives (f_{runoff} and $f_{\text{NH}_4\text{-N}}$) as

$$\begin{cases} f_{\text{runoff}} = \min[(|\text{bias}| + 2 - r - NS)/3] \\ f_{\text{NH}_4\text{-N}} = \min[(|\text{bias}| + 1 - r)/2] \end{cases} \quad (1)$$

because the case study was only a demonstration of the model performance.

Moreover, because of the high regulation in most rivers, it is necessary to consider the impact of dam regulation in the integrated water system models. The dam and sluice regulation usually disturbs the intra-annual distribution of flow events, e.g., flattening high flow and increasing low flow. The simulation performances of high and low flow were evaluated separately, and the effectiveness of the DRM was tested by comparing the simulation with and without considering the regulation. The high and low flow was determined by cumulative distribution function (CDF) and the threshold of 50% was used for easy presentation, that is, the flow was treated as high flow (or low flow) if its percentile was greater than (or smaller than) the threshold.

3 Results and discussion

3.1 Parameter sensitivity analysis

Nine sensitive parameters were detected for runoff simulation (Table 3), including soil related parameters W_{fc} (field capacity), W_{sat} (saturated moisture capacity), K_r (interflow

yield coefficient) and K_{sat} (steady state infiltration rate); TVGM parameters g_1 (basic surface runoff coefficient) and g_2 (influence coefficient of soil moisture) for surface runoff calculation; ground water recharge parameters K_g (baseflow yield coefficient) and T_g (delay time for aquifer recharge); and adjusted factor K_{ET} of evapotranspiration.

5 All these parameters controlled the main hydrological processes, in which soil water and evapotranspiration processes were distinctly important, explaining 54.3 and 23.2 % of the runoff variation, respectively.

For $\text{NH}_4\text{-N}$ concentration simulation, more than 90 % of observed $\text{NH}_4\text{-N}$ concentration variation were explained by 14 sensitive parameters which were categorized into hydrological (59.28 % of variation), $\text{NH}_4\text{-N}$ (20.65 % of variation) and COD (12.34 % of variation) related parameters. The main explanations were that hydrological processes provided the hydrological boundaries which affected the nonpoint source pollutant load into rivers, the degradation and settlement processes of $\text{NH}_4\text{-N}$ in water bodies (rivers and reservoirs) (van Griensven et al., 2002). $\text{NH}_4\text{-N}$ concentration was further influenced by the settling and biological oxidation processes. Moreover, it was a competitive relationship between COD and $\text{NH}_4\text{-N}$ to consume DO of water bodies in a certain limited level (Brown and Barnwell, 1987).

3.2 Hydrological simulation

10 The simulations fitted the observations well at all the stations from the midstream to downstream (Fig. 7 and Table 4). The biases were very close to 0.0 at all the regulated stations except Zhoukou with the underestimation (0.24 for calibration and 0.41 for validation) and Luohe with overestimation (-0.52 for validation). The reason of the obvious biases was that the calibration was to obtain the optimal solution for the average of three evaluation indices, rather than the bias only. The r values ranged from 0.75 (Luohe for validation) to 0.92 (Yingshang for calibration) with the average value of 0.85 while the NS values ranged from 0.51 (Luohe for validation) to 0.84 (Yingshang for calibration) with the average value of 0.70. The results of the regulated stations were little worse than those of the less-regulated station (Shenqiu) due to the regulation.

HESSD

12, 4997–5053, 2015

Integrated water system simulation

Y. Y. Zhang et al.

Title Page

Abstract

Introduction

Conclusions

References

Tables

Figures

⏪

⏩

◀

▶

Back

Close

Full Screen / Esc

Printer-friendly Version

Interactive Discussion



Integrated water
system simulation

Y. Y. Zhang et al.

Title Page

Abstract

Introduction

Conclusions

References

Tables

Figures

◀

▶

◀

▶

Back

Close

Full Screen / Esc

Printer-friendly Version

Interactive Discussion



By comparing the simulation results with the observations from 2003 to 2008, we can see that the high and low flows were usually overestimated at all the stations if the model did not consider the regulations (Fig. 8). Except the high flow events at Zhoukou, both high and low flow events at all the stations were simulated better when the dam and sluice regulation was considered (Table 5). The best fitting was at Fuyang, especially for the high flow simulation (bias = 0.10, $r = 0.89$ and NS = 0.78). From unregulation to regulation settings, the improvements measured by f_{runoff} ranged from -0.08 (Zhoukou) to -0.29 (Huaidian) for high flow simulation, from -0.05 (Zhoukou) to -0.31 (Huaidian) for average flow simulation, and from -1.97 (Fuyang) to -3.91 (Yingshang) for low flow simulation except Zhoukou (1.28). The improvements of simulation performance of low flows were the most obvious. However, their performance still need to be improved further, especially the underestimation at Zhoukou and Huaidian. The possible reasons were that, on the one hand, the applied evaluation indices (r and NS) are known to emphasize on the high flows and are disadvantageous to evaluate the low flow simulation (Pushpalatha et al., 2012) and the objective of autocalibration was to obtain the optimal solution for the average of three evaluation indices, rather than the bias only. The slightly sacrifice of bias improved the overall simulation performance evaluated by these three indices. On the other hand, the dam regulation module is still not able to fully capture the low flow events.

In addition, the model performances of monthly flows were even better, particular for r and NS. The values of r ranged from 0.87 (Luohe for both calibration and validation) to 0.95 (Fuyang for calibration) with the mean of 0.92, while the values of NS ranged from 0.67 (Luohe for validation) to 0.94 (Shenqiu for validation) with the mean of 0.80. Zhang et al. (2013) reproduced the long-term monthly flows by SWAT at the same stations. In comparison with the existing results, the extended model improved the flow simulations at the downstream stations although it became little worse at the upstream stations (Luohe and Zhoukou for calibration). In particular, the water volume and agreements with the observations (i.e., bias and NS) were well captured.

3.3 Water quality simulation

The simulated concentrations matched well with the observations according to the evaluation standard recommend by Moriasi et al. (2007) (Fig. 9 and Table 6). The r values of all the stations were over 0.60 expect Zhoukou (0.56 for validation), Yingshang (0.49 for validation) and Shenqiu (0.41 for validation) with the average value of 0.67. The bias of all the stations were considered as “acceptable” with the range from -0.27 (Fuyang for validation) to 0.29 (Zhoukou for calibration). The best simulation was at Luohe. The obvious discrepancies between the simulation and observation often appeared in the period from January to May because of the poor simulation performance of low flows.

The simulation was also significantly improved when the regulation was considered in comparison with the results without the consideration of regulation, except at Fuyang for calibration. The decreases of $f_{\text{NH}_4\text{-N}}$ value ranged from 0.10 (Huaidian for calibration) to 0.49 (Zhoukou for validation) although it was increased slightly at Fuyang for calibration (0.02). The regulation of dams and sluices played a critical role in the water quality simulation. In the upperstream of Shaying River, the flow was small and the pollutant concentration reduced obviously, due to the degradation and settlement of large water storage. In the downstream of Shaying River, the pollutant concentration increased due to the pollutant accumulation and the decreasing of flow by the regulation of dams and sluices (Zhang et al., 2010). Therefore, the simulated concentrations without regulation were usually overestimated or greater than the simulation with regulation at the upperstream stations (Luohe and Zhoukou), but they were underestimated at the downstream stations (Huaidian, Fuyang and Yingshang). The largest difference of simulation between with and without the regulation consideration appeared at Zhoukou.

The spatial pattern of average annual nonpoint source $\text{NH}_4\text{-N}$ loads was shown in Fig. 10a. The modeled annual yield rates ranged from $0.048 \text{ t km}^{-2} \text{ year}^{-1}$ to $11.00 \text{ t km}^{-2} \text{ year}^{-1}$ with the average value of $0.73 \text{ t km}^{-2} \text{ year}^{-1}$. The yield of each administrative region was summarized from the subbasin scale according to the area percentage of subbasins in each administrative region. In comparison with the statistical

HESSD

12, 4997–5053, 2015

Integrated water system simulation

Y. Y. Zhang et al.

Title Page

Abstract

Introduction

Conclusions

References

Tables

Figures

◀

▶

◀

▶

Back

Close

Full Screen / Esc

Printer-friendly Version

Interactive Discussion



Integrated water
system simulation

Y. Y. Zhang et al.

Title Page

Abstract

Introduction

Conclusions

References

Tables

Figures

◀

▶

◀

▶

Back

Close

Full Screen / Esc

Printer-friendly Version

Interactive Discussion



load of each administrative region which estimated based on the soil erosion, landuse and fertilizer amount in the official report (Wang, 2011), the bias of simulated nonpoint source load in the whole region was 21.31 % when the two regions with great bias (i.e., Fuyang and Pingdingshan) were excluded as the outliers. The high load yield regions were in the middle of Pingdingshan, Xuchang, Zhengzhou, Fuyang and Zhoukou regions. The spatial pattern was significantly correlated with the distribution of paddy area ($r = 0.506$, $p < 0.001$) and rice yield ($r = 0.799$, $p < 0.001$) (Fig. 10b and c). The fertilizer loss in the paddy areas might be the primary contributor to the nonpoint source $\text{NH}_4\text{-N}$ load, possibly because the average nitrogen loss coefficient in China was just 30 ~ 70 % in the paddy areas, which was greater than that in the dry areas (20 ~ 50 %) (Zhu, 2000; Xing and Zhu, 2000).

The observed average annual point source $\text{NH}_4\text{-N}$ loads into rivers were about $4.70 \times 10^4 \text{ t year}^{-1}$ in the Shaying River Catchment, which were summarized from the collected data for model input. The nonpoint source load contributed 18.66 % of the overall $\text{NH}_4\text{-N}$ load on average from 2003 to 2005, which was little less than the statistical results (29.37 %) given in the official report (Wang, 2011). Moreover, the contributions of non-point source load at the stations ranged from 31.72 (Huaidian) to 47.13 % (Shenqiu). In comparison with the nonpoint source load of each administrative region in 2000, the simulated annual loads tended to decrease from 2003 to 2005 except in Luoyang and Pingdingshan regions. The decrease rate in the entire region was 26.30 %. The primary pollution source in the Shaying River Catchment was still the point source, but the non-point source was also of great concern and its spatial characteristic was that the contribution of nonpoint source was greatest in the upstream, and was lowest in the middle and downstream because the point source load emission was usually concentrated in the this region. Therefore, in comparison with the results of Zhang et al. (2013), the overall simulation performance of $\text{NH}_4\text{-N}$ concentration was also improved greatly by considering the detailed processes of nutrient in the soil layers.

3.4 Crop yield simulation

The simulated corn yield and its spatial pattern were shown in Fig. 11. The average annual yields were summarized at subbasin scale and ranged from 0.08 to 326.95 t km⁻² year⁻¹ with the average value of 76.84 t km⁻² year⁻¹. The yield of each administrative region was further summarized and compared with the data from statistical yearbooks from 2003 to 2005 (Henan Statistical Yearbook, 2003, 2004 and 2005) to test the simulation performance (See the inset of Fig. 11). The high-yield regions were Luohe, Fuyang and Zhoukou in the middle and down reaches, whose primary land use were dry land (93.12, 95.87 and 93.18 %, respectively). The yields of Luohe, Nanyang, Kaifeng regions were well simulated. The total yield was underestimated in the whole basin with the bias of 19.93%. The discrepancies might be caused by the boundary mismatch between the administrative region and subbasin, obvious spatial heterogeneities of human agricultural activities, and the inaccurate cropping patterns in such huge region. Higher resolution remote sensing image and field investigation might improve the model performance.

4 Conclusions

In this study, an integrated water system model was developed on the basis of TVGM hydrological model to address water issues emerged in the complex basins and the model performance was demonstrated in the Shaying River Catchment of China by comparing with the observations of several key components of major processes, such as runoff, water quality concentrations, nonpoint source pollutant load and crop yield.

The extended model integrates multi-scale processes and their interactions at the field, subbasin scales into a unified system using the two critical and inseparable linkages, e.g. water and nutrient (N, P and C). The model provides a reasonable tool for the effective water governance by capturing some indicative components of water related subsystems simultaneously including the hydrological components (e.g., soil

HESSD

12, 4997–5053, 2015

Integrated water system simulation

Y. Y. Zhang et al.

Title Page

Abstract

Introduction

Conclusions

References

Tables

Figures

⏪

⏩

⏴

⏵

Back

Close

Full Screen / Esc

Printer-friendly Version

Interactive Discussion



Integrated water system simulation

Y. Y. Zhang et al.

Title Page

Abstract

Introduction

Conclusions

References

Tables

Figures

I◀

▶I

◀

▶

Back

Close

Full Screen / Esc

Printer-friendly Version

Interactive Discussion



water and evaporation, plant transpiration, runoff and water storage in the dams and sluices), water quality components (e.g., nonpoint source nutrient load, water quality concentrations in water bodies), as well as ecological components (crop yield) which could be calibrated if the observations are available. The case study has shown that the simulated runoffs at most stations fitted the observations well in the highly regulated Shaying River Catchment. All the evaluation criteria were acceptable for both the daily and monthly simulations except at one or two stations. This model captured the variation of discontinuous daily $\text{NH}_4\text{-N}$ concentration and properly simulated the spatial patterns of nonpoint source pollutant load and corn yield.

Due to the heterogeneity of spatial data in large basins and insufficient observations of every subsystems, not all the results were acceptable and several processes were still not well calibrated (low flow events, nonpoint source pollutant load and crop yield, etc.). The model could be improved by further exploring the water related processes. More complex humanity activities and water-related processes in the agricultural management, urban area and economy system will be incorporated into this model once the interaction mechanisms with natural hydrologic cycle could be depicted accurately. Additionally, there are still several great challenges in the combined calibration of multi-component and model uncertainty analysis because of the interactions and tradeoffs among different processes. The over-parameterization and the reasonable initial conditions of parameters need also be treated carefully in applications. Advanced mathematic analysis technologies should be applied in the future works, such as multi-objective optimization algorithm.

Appendix A: Hydrological cycle module

The basic water balance equation is

$$P_i + \text{SW}_i = \text{SW}_{i+1} + \text{Rs}_i + \text{Ea}_i + \text{Rss}_i + \text{Rg}_i + \text{In}_i \quad (\text{A1})$$

where P is precipitation (mm); SW is soil water moisture (mm); E_a is actual evapotranspiration (mm) including soil evaporation (E_s , mm) and plant transpiration (E_p , mm); R_s , R_{ss} and R_g is surface runoff, interflow and baseflow (mm), respectively; ln is the vegetation interception (mm) and i is the time step (day).

E_s and E_p are determined by potential evapotranspiration (E_0 , mm), leaf area index (LAI, $m^2 m^{-2}$) and surface soil residues (rsd , tha^{-1}) (Ritchie, 1972) as.

$$\begin{cases} E_a = E_t + E_s \leq E_0 \\ E_p = \begin{cases} LAI \cdot E_0 / 3 & 0 \leq LAI \leq 3.0 \\ E_0 & LAI > 3.0 \end{cases} \\ E_s = E_0 \cdot \exp(-5.0 \times 10^{-5} \cdot rsd) \end{cases} \quad (A2)$$

where E_0 is calculated by Hargreaves method (Hargreaves and Samani, 1982).

The surface runoff (R_s , mm) yield equation (TVGM; Xia et al., 2005) is given as

$$R_s = g_1 (SW_u / W_{sat})^{g_2} \cdot (P - ln) \quad (A3)$$

where SW_u and W_{sat} are surface soil moisture and saturation moisture (mm), respectively; g_1 and g_2 are coefficients of basic runoff and soil moisture, respectively.

The interflow (R_{ss} , mm) and baseflow (R_g , mm) are considered as a linear storage-outflow relationship (Wang et al., 2009) as

$$\begin{cases} R_{ss} = k_r \cdot SW_u \\ R_g = k_g \cdot SW_l \end{cases} \quad (A4)$$

where k_r and k_g are the yield coefficients of interflow and baseflow, respectively; SW_l is soil moisture of lower layer (mm).

The infiltration from the upper to lower soil layer is calculated using storage routing methodology (Neitsch et al., 2011) as

$$\begin{cases} W_{inf} = (SW_u - W_{fc}) \cdot [1 - \exp(-t/T_{inf})] \\ T_{inf} = (W_{sat} - W_{fc}) / K_{sat} \end{cases} \quad (A5)$$

where W_{inf} is water infiltration amount on a given day (mm); W_{fc} is soil field capacity (mm); t and T_{inf} are time step and travel time for infiltration (hrs), respectively; and K_{sat} is saturated hydraulic conductivity (mm h^{-1}).

The calculation of overland flow routing is adopted from Neitsch et al. (2011) as

$$\begin{cases} Q_{\text{overl}} = (Q'_{\text{overl}} + Q_{\text{stor},i-1}) \cdot [1 - \exp(-T_{\text{retain}}/T_{\text{route}})] \\ T_{\text{route}} = T_{\text{overl}} + T_{\text{rch}} = \frac{L_{\text{overl}} \cdot n_{\text{overl}}^{0.6}}{18 \cdot \text{slp}_{\text{overl}}^{0.3}} + \frac{0.62 \cdot L_{\text{rch}} \cdot n_{\text{rch}}^{0.75}}{A^{0.125} \cdot \text{slp}_{\text{rch}}^{0.375}} \end{cases} \quad (\text{A6})$$

where Q_{overl} is the overland flow discharged into main channel (mm); Q'_{overl} is the lateral flow amount generated in the subbasin (mm), $Q_{\text{stor},i-1}$ is the lateral flow in the previous day (mm); T_{retain} is the retain time of flow (days); T_{route} , T_{overl} and T_{rch} are the routing times of the total flow, overland flow and river flow, respectively (days); L_{overl} and L_{rch} are the lengths of subbasin slope and river, respectively (km); $\text{slp}_{\text{overl}}$ and slp_{rch} are the slopes of subbasin and river, respectively (m m^{-1}); n_{overl} and n_{rch} are the Manning's roughness coefficients for subbasin and river, respectively (m m^{-1}); A is the subbasin area (km^2).

Appendix B: Soil biochemical module

B1 Soil temperature (Williams et al., 1984)

$$T(Z, t) = \bar{T} + (\text{AM}/2 \cdot \cos[2\pi \cdot (t - 200)/365] + \text{TG} - T(0, t)) \cdot \exp(-Z/\text{DD}) \quad (\text{B1})$$

where Z is soil depth (mm); t is time step (days); \bar{T} and TG are average annual temperature and surface temperature ($^{\circ}\text{C}$), respectively; AM is the annual variation amplitude

HESSD

12, 4997–5053, 2015

Integrated water system simulation

Y. Y. Zhang et al.

Title Page

Abstract

Introduction

Conclusions

References

Tables

Figures

◀

▶

◀

▶

Back

Close

Full Screen / Esc

Printer-friendly Version

Interactive Discussion



of daily temperature; DD is the damping depth of soil temperature (mm) given as

$$\begin{cases} DD = DP \cdot \exp\left\{\ln(500/DP) \cdot [(1 - \xi)/(1 + \xi)]^2\right\} \\ DP = 1000 + 2500BD/[BD + 686 \exp(-5.63BD)] \\ \xi = SW/[(0.356 - 0.144BD) \cdot Z_M] \\ TG_{IDA} = (1 - AB) \cdot (T_{mx} + T_{mn})/2 \cdot (1 - RA/800) + T_{mx} \cdot RA/800 + AB \cdot TG_{IDA-1} \end{cases} \quad (B2)$$

where DP is maximum damping depth of soil temperature (mm); BD is soil bulk density (t m^{-3}); ξ is scale parameter; IDA is day of the year; AB is surface albedo; RA is daily solar radiation (ly).

B2 C and N cycle (Li et al., 1992)

Decomposition. The decomposition of resistant and labile C is described by the first order kinetic equation, viz.

$$dC/dt = \mu_{\text{CLAY}} \cdot \mu_{\text{C:N}} \cdot \mu_{t,n} \cdot [S \cdot k_1 + (1 - S) \cdot k_2] \quad (B3)$$

where μ_{CLAY} , $\mu_{\text{C:N}}$ and $\mu_{t,n}$ is the reduction factor of clay content, C : N ratio and temperature for nitrification, respectively; S is labile fraction of organic C compounds; k_1 and k_2 is specific decomposition rate of labile fraction and resistant fraction, respectively (day^{-1}).

The ammonia amount absorbed by clay and organic matters (FIX_{NH_4}) is estimated using equation

$$\text{FIX}_{\text{NH}_4} = [0.41 - 0.47 \cdot \log(\text{NH}_4)] \cdot (\text{CLAY}/\text{CLAY}_{\text{max}}) \quad (B4)$$

where NH_4 is NH_4^+ concentration in the soil liquid (g kg^{-1}). CLAY and CLAY_{max} are clay content and the maximum clay content, respectively.

$$\begin{cases} \log(K_{\text{NH}_4}/K_{\text{H}_2\text{O}}) = \log(\text{NH}_{4m}/\text{NH}_{3m}) + \text{pH} \\ \text{NH}_{3m} = 10^{\{\log(\text{NH}_4) - \log(K_{\text{NH}_4}) - \log(K_{\text{H}_2\text{O}}) + \text{pH}\}} \cdot (\text{CLAY}/\text{CLAY}_{\text{max}}) \\ \text{AM} = 2 \cdot (\text{NH}_3) \cdot (D \cdot t/3.14)^{0.5} \end{cases} \quad (B5)$$

where K_{NH_4} and $K_{\text{H}_2\text{O}}$ are dissociation constants for $\text{NH}_4^+ : \text{NH}_3$ equilibrium, $\text{H}^+ : \text{OH}^-$ equilibrium, respectively; $\text{NH}_{4,m}$ and $\text{NH}_{3,m}$ are NH_4^+ and NH_3 concentrations (mol L^{-1}) in the liquid phase, respectively; AM and D are accumulated NH_3 loss (mol cm^{-2}) and diffusion coefficients (cm^2/d^2), respectively.

The nitrification rate (dNNO , kg/ha/day) is a function of the available NH_4^+ , soil temperature and soil moisture. N_2O emission is a function of soil temperature and soil NH_4^+ concentration, viz.:

$$\begin{cases} \text{dNNO} = \text{NH}_4(t) \cdot [1 - \exp(-K_{35} \cdot \mu_{t,n} \cdot dt)] \cdot \mu_{\text{SW},n} \\ \text{N}_2\text{O} = (0.0014 \cdot \text{NH}_4/30.0) \cdot (0.54 + 0.51 \cdot T)/15.8 \end{cases} \quad (\text{B6})$$

where $\text{NH}_4(t)$ is the available NH_4^+ (kg ha^{-1}); K_{35} is the nitrification rate at 35°C ($\text{mg kg}^{-2} \text{ha}^{-1}$); $\mu_{\text{SW},n}$ is soil water moisture adjusted factor for nitrification.

Denitrification. The growth rate of denitrifier is proportional to their respective biomass, which is calculated with double Monod kinetics equation

$$\begin{cases} (dB/dt)_g = \mu_{\text{DN}} \cdot B(t) \\ \mu_{\text{DN}} = \mu_{t,dn} \cdot (u_{\text{NO}_3} \cdot \mu_{\text{PHNO}_3} + u_{\text{NO}_2} \cdot \mu_{\text{PHNO}_2} + u_{\text{N}_2\text{O}} \cdot \mu_{\text{PHN}_2\text{O}}) \\ u_{\text{N}_x\text{O}_y} = u_{\text{N}_x\text{O}_y,\text{max}} \cdot (C/K_{\text{C},1/2} + C) \cdot (\text{N}_x\text{O}_y/K_{\text{N}_x\text{O}_y,1/2} + \text{N}_x\text{O}_y) \end{cases} \quad (\text{B7})$$

where B is the denitrifier biomass (kg); $(dB/dt)_g$ is the potential growth rate of denitrifier biomass ($\text{kg ha}^{-1} \text{day}^{-1}$); μ_{DN} is the relative growth rate of the denitrifiers; $u_{\text{N}_x\text{O}_y}$ and $u_{\text{N}_x\text{O}_y,\text{max}}$ are the relative and maximum growth rates of NO_2^- , NO_3^- and N_2O denitrifiers. $K_{\text{C},1/2}$ and $K_{\text{N}_x\text{O}_y,1/2}$ are the half velocity constants of C and N_xO_y , respectively. $\mu_{\text{PHN}_x\text{O}_y}$ and $\mu_{t,dn}$ are the reduction factors of soil pH and temperature, respectively, and are

HESSD

12, 4997–5053, 2015

Integrated water system simulation

Y. Y. Zhang et al.

Title Page

Abstract

Introduction

Conclusions

References

Tables

Figures

◀

▶

◀

▶

Back

Close

Full Screen / Esc

Printer-friendly Version

Interactive Discussion



given as

$$\begin{cases} \mu_{\text{PHNO}_3} = 7.14 \cdot (\text{pH} - 3.8)/22.8 \\ \mu_{\text{PHNO}_2} = 1.0 \\ \mu_{\text{PHN}_2\text{O}} = 7.22 \cdot (\text{pH} - 4.4)/18.8 \\ \mu_{t,dn} = \begin{cases} 2^{(T-22.5)/10} & \text{if } T < 60^\circ\text{C} \\ 0 & \text{if } T \geq 60^\circ\text{C} \end{cases} \end{cases} \quad (\text{B8})$$

The death rate of denitrifier $(dB/dt)_d$ ($\text{kg ha}^{-1} \text{h}^{-1}$) is proportional to denitrifier biomass, viz.

$$5 \quad (dB/dt)_d = M_C \cdot Y_C \cdot B(t) \quad (\text{B9})$$

where M_C and Y_C are maintenance coefficient of C (1 h^{-1}), maximum growth yield of soluble C ($\text{kg ha}^{-1} \text{h}^{-1}$), respectively.

The consumption rates of soluble C and CO_2 production are calculated as

$$\begin{cases} dC_{\text{con}}/dt = (\mu_{\text{DN}}/Y_C + M_C) \cdot B(t) \cdot \mu_{\text{SW},d} \\ d\text{CO}_2/dt = dC_{\text{con},t}/dt - (dB/dt)_d \end{cases} \quad (\text{B10})$$

10 where $\mu_{\text{SW},d}$ is soil water moisture adjusted factor for denitrification.

The NO_3^- , NO_2^- , NO and N_2O consumption are calculated as

$$dN_{xO_y}/dt = (u_{N_xO_y}/Y_{N_xO_y} + M_{N_xO_y} \cdot N_{xO_y}/N) \cdot B(t) \cdot \mu_{\text{PHN}_xO_y} \cdot \mu_{t,dn} \quad (\text{B11})$$

where $M_{N_xO_y}$ and $Y_{N_xO_y}$ are maintenance coefficient (1 h^{-1}), maximum growth yield on NO_3^- , NO_2^- , NO or N_2O ($\text{kg ha}^{-1} \text{h}^{-1}$), respectively.

15 N assimilation is calculated on the basis of the growth rates of denitrifiers and the C : N ratio ($\text{CNR}_{\text{D:N}}$) in the bacteria, viz.

$$(dN/dt)_{\text{ass}} = (dB/dt)_g \cdot (1/\text{CNR}_{\text{D:N}}) \quad (\text{B12})$$

The emission rates are the functions of adsorption coefficients of the gases in soils and to the air filled porosity of the soil, given as.

$$\begin{cases} P(N_2) = 0.017 + (0.025 - 0.0013 \cdot AD) \cdot PA \\ P(N_2O) = [30.0 \cdot (0.0006 + 0.0013 \cdot AD) + (0.013 - 0.005 \cdot AD)] \cdot PA \\ P(NO) = 0.5 \cdot [(0.0006 + 0.0013 \cdot AD) + (0.013 - 0.005 \cdot AD) \cdot PA] \end{cases} \quad (B13)$$

where $P(N_2)$, $P(NO)$ and $P(N_2O)$ are the emission rates of N_2 , NO , N_2O , respectively, during a day; PA and AD are the air-filled fraction of the total porosity and adsorption factor depending on clay content in the soil, respectively.

Nitrate leaching. The NO_3^-N leaching rate is a function of clay content, organic C content and water infiltration in the soil layer as

$$Leach_{NO_3} = W_{inf} \cdot \mu_{CLAY} \cdot \mu_{SOC} \quad (B14)$$

where $Leach_{NO_3}$ is the NO_3^-N leaching rate; μ_{CLAY} and μ_{SOC} are the influence coefficients of clay content and organic C in the soil layer, respectively.

B3 P cycle

The descriptions of P mineralization, decomposition and sorption are adopted from Neitsch et al. (2011) and provided as the supplementary material.

Appendix C: Dam regulation module (Zhang et al., 2013)

The water balance model is used to consider the inflow, outflow, precipitation, evapotranspiration and seepage of dam or sluice. The equation is:

$$\Delta V = V_{flowin} - V_{flowout} + V_{pcp} - V_{evap} - V_{seep} \quad (C1)$$

where ΔV , V_{flowin} and $V_{flowout}$ are the water storage variation, water volumes of entering and flowing out, respectively (m^3), and are calculated by HCM; V_{pcp} , V_{evap} and V_{seep} are

Title Page

Abstract

Introduction

Conclusions

References

Tables

Figures

⏪

⏩

◀

▶

Back

Close

Full Screen / Esc

Printer-friendly Version

Interactive Discussion



the precipitation, evaporation and seepage volume, respectively (m^3), which are the functions of water surface area and vary with water storage.

According to the design data of dams and sluices in China, there is a particular relationship among water level, storage volume and outflow. The water discharge is determined by the water level or water storage volume. Thus, the relationships are described by equations.

$$\begin{cases} V_{\text{flowout}} = f'(V, H) \\ SA = f''(V, H) \end{cases} \quad (\text{C2})$$

where V and H are the water storage volume and water level during a day, respectively; f' and f'' are the functions which could be determined by statistical analysis methods (e.g., correlation analysis, linear or non-linear regression analysis, polynomial regression analysis and least squares fitting).

Appendix D: Evaluation indices of model performance

Bias:

$$\text{bias} = \frac{\sum_{i=1}^N (O_i - S_i)}{\sum_{i=1}^N O_i} \quad (\text{D1})$$

Relative error:

$$\text{re} = \sum_{i=1}^N \frac{O_i - S_i}{O_i} \times 100\% \quad (\text{D2})$$

Root mean square error:

$$\text{RMSE} = \sqrt{\sum_{i=1}^N (O_i - S_i)^2 / N} \quad (\text{D3})$$

Title Page

Abstract

Introduction

Conclusions

References

Tables

Figures

⏪

⏩

◀

▶

Back

Close

Full Screen / Esc

Printer-friendly Version

Interactive Discussion



Correlation coefficient:

$$r = \frac{\sum_{i=1}^N (O_i - \bar{O}) \cdot (S_i - \bar{S})}{\sqrt{\sum_{i=1}^N (O_i - \bar{O})^2 \cdot \sum_{i=1}^N (S_i - \bar{S})^2}} \quad (D4)$$

Coefficient of efficiency:

$$NS = 1 - \frac{\sum_{i=1}^N (O_i - S_i)^2}{\sum_{i=1}^N (O_i - \bar{O})^2} \quad (D5)$$

5 where O_i and S_i are the i th observed and simulated values, respectively; \bar{O} and \bar{S} are the average observed and simulated values, respectively. N is the length of series.

**The Supplement related to this article is available online at
doi:10.5194/hessd-12-4997-2015-supplement.**

10 *Acknowledgements.* This study was supported by the Natural Science Foundation of China (No. 41271005), the Key Project for the Strategic Science Plan in IGSNRR, CAS (No. 2012ZD003), the Endeavour Research Fellowship, China Visiting Scholar Project from China Scholarship Council and CSIRO Computational and Simulation Sciences Research Platform. Thanks to Yongqiang Zhang, Mr. James R Frankenberger during our internal review procedure, the editor (Christian Stamm) and two anonymous reviewers for their valuable comments which
15 helped improving the quality and presentation of the manuscript.

References

- Abbott, M. B., Bathurst, J. C., Cunge, J. A., O'Connell, P. E., and Rasmussen, J.: An introduction to the european system: systeme hydrologique European (SHE), *J. Hydrol.*, 87, 61–77, 1986.
- 20 Arthington, A. H.: *Environmental Flows: Saving Rivers in the Third Millennium*, University of California Press, Berkeley, CA, 406 pp., 2012.

Title Page

Abstract

Introduction

Conclusions

References

Tables

Figures

⏪

⏩

◀

▶

Back

Close

Full Screen / Esc

Printer-friendly Version

Interactive Discussion



Integrated water system simulation

Y. Y. Zhang et al.

Title Page

Abstract

Introduction

Conclusions

References

Tables

Figures

|◀

▶|

◀

▶

Back

Close

Full Screen / Esc

Printer-friendly Version

Interactive Discussion



- Arnold, J. G., Srinivasan, R., Muttiah, R. S., and Williams, J. R.: Large-area hydrologic modeling and assessment: Part I, model development, *J. Am. Water Resour. As.*, 34, 73–89, 1998.
- Beven, K. J. and Kirkby, M. J.: A physically based variable contributing area model of basin hydrology, *Hydrol. Sci. Bull.*, 24, 43–69, 1979.
- 5 Brakensiek, D. L. Estimating the effective capillary pressure in the green and ampt infiltration equation, *Water Resour. Res.*, 13, 680–682, 1977.
- Bicknell, B. R., Imhoff, J. C., Kittle, J. L., Donigian, A. S., and Johanson, R. C.: Hydrologic Simulation Program – FORTRAN (HSPF): User's Manual for Release, 10. Report No. EPA/600/R-93/174, Athens, Ga., US EPA Environmental Research Lab, 1993.
- 10 Biswas, A. K.: Integrated water resources management: a reassessment – a water forum contribution, *Water Int.*, 29, 248–256, 2004.
- Blöschl, G. and Sivapalan, M.: Scale issues in hydrological modelling: a review, *Hydrol. Process.*, 9, 251–290, 1995.
- Borah, D. K. and Bera, M.: Watershed-scale hydrologic and nonpoint-source pollution models: review of application, *Trans. ASAE*, 47, 789–803, 2004.
- 15 Bouraoui, F. and Dillaha, T. A.: ANSWERS-2000: runoff and sediment transport model, *J. Environ. Eng.*, 122, 493–502, 1996.
- Brown, L. C. and Barnwel, T. O.: The enhanced stream water quality models QUAL2E and QUAL2E-UNCAS: documentation and user manual, *Env. Res. Laboratory. US EPA*, 1987.
- 20 Burt, T. P. and Pinay, G.: Linking hydrology and biogeochemistry in complex landscapes, *Prog. Phys. Geog.*, 29, 297–316, 2005.
- Chen, Y., Song, X., Zhang, Z., Shi, P., and Tao, F.: Simulating the impact of flooding events on non-point source pollution and the effects of filter strips in an intensive agricultural watershed in China, *Limnology*, 16, 91–101, doi:10.1007/s10201-014-0443-2, 2015.
- 25 China's national standard (CNS): Current land use condition classification (GB/T21010-2007), General administration of quality supervision, inspection and quarantine of China and Standardization administration of China, Beijing, China, 2007.
- China State Environmental Protection Administration (CSEPA): Environmental quality standards for surface water – GB 3838-2002m, China Environmental Science Press, Beijing, 2002.
- 30 Deng, J., Zhu, B., Zhou, Z. X., Zheng, X. H., Li, C. S., Wang, T., and Tang, J. L.: Modeling nitrogen loadings from agricultural soils in southwest China with modified DNDC, *J. Geophys. Res.-Biogeo.*, 116, 2005–2012, 2011.

HESSD

12, 4997–5053, 2015

Integrated water system simulation

Y. Y. Zhang et al.

[Title Page](#)[Abstract](#)[Introduction](#)[Conclusions](#)[References](#)[Tables](#)[Figures](#)[|◀](#)[▶|](#)[◀](#)[▶](#)[Back](#)[Close](#)[Full Screen / Esc](#)[Printer-friendly Version](#)[Interactive Discussion](#)

- Di Toro, D. M., Fitzpatrick, J. J., and Thomann, R. V.: Water quality analysis simulation program (WASP) and model verification program (MVP)-Documentation, MN, Contract No. 68-01-3872, Hydrosience, Inc., Westwood, NY, for US EPA, Duluth, 1983.
- Duan, Q., Sorooshian, S., and Gupta, V. K.: Optimal use of the SCE-UA global optimization method for calibrating watershed models, *J. Hydrol.*, 158, 265–284, 1994.
- Efstratiadis, A. and Koutsoyiannis, D.: One decade of multi-objective calibration approaches in hydrological modelling: a review, *J. Hydrol.*, 55, 58–78, 2010.
- Gassman, P. W., Reyes, M. R., Green, C. H., and Arnold, A. G.: The soil and water assessment tool: historical development, applications, and future research directions, *T. ASABE*, 50, 1211–1250, 2007.
- Gleick, P. H.: Water in crisis: paths to sustainable water use, *Ecol. Appl.*, 8, 571–579, 1998.
- Goldberg, D. E.: Genetic algorithms in search, optimization, and machine learning, Reading Menlo Park: Addison-Wesley, Massachusetts, USA, 1989.
- Hamrick, J. M.: A three-dimensional environmental fluid dynamics computer code: theoretical and computational aspects, Special Report, The College of William and Mary, Virginia Institute of Marine Science, Virginia, USA, 317, 1992.
- Hargreaves, G. H. and Samani, Z. A.: Estimating potential evapotranspiration, *J. Irrigat. Drain. Div.*, 108, 225–230, 1982.
- Henan Statistical Yearbook, China Statistics Press, Beijing, 2003.
- Henan Statistical Yearbook, China Statistics Press, Beijing, 2004.
- Henan Statistical Yearbook, China Statistics Press, Beijing, 2005.
- Hering, J. G., Hoehn, E., Klinke, A., Maurer, M., Peter, A., Reichert, P., Robinson, C., Schirmer, K., Schirmer, M., Stamm, C., and Wehrli, B.: Moving targets, long-lived infrastructure, and increasing needs for integration and adaptation in water management: an illustration from Switzerland, *Environ. Sci. Technol.*, 46, 112–118, 2012.
- Horst, W. J., Kamh, M., Jibrin, J. M., and Chude, V. O.: Agronomic measures for increasing P availability to crops, *Plant Soil*, 237, 211–223, 2001.
- Johnes, P. J.: Evaluation and management of the impact of land use change on the nitrogen and phosphorus load delivered to surface waters: the export coefficient modelling approach, *J. Hydrol.*, 183, 323–349, 1996.
- Jordan, Y. C., Ghulam, A., and Hartling, S.: Traits of surface water pollution under climate and land use changes: a remote sensing and hydrological modeling approach, *Earth-Sci. Rev.*, 128, 181–195, 2014.

Integrated water system simulation

Y. Y. Zhang et al.

Title Page

Abstract

Introduction

Conclusions

References

Tables

Figures

⏪

⏩

◀

▶

Back

Close

Full Screen / Esc

Printer-friendly Version

Interactive Discussion



Kirchner, J. W.: Getting the right answers for the right reasons: linking measurements, analyses, and models to advance the science of hydrology, *Water Resour. Res.*, 42, W03S04 doi:10.1029/2005WR004362, 2006.

Kindler, J.: Integrated water resources management: the meanders, *Water Int.*, 25, 312–319, 2000.

King, K. W., Arnold, J. G., and Bingner, R. L.: Comparison of Green–Ampt and curve number methods on Goodwin Creek watershed using SWAT. *Trans. ASAE*, 42, 919–925, 1999.

Kennedy, J.: Particle swarm optimization, *Encyclopedia of Machine Learning*. Springer USA, 760–766, 2010.

Li, C., Frohling, S., and Frohling, T. A.: A model of nitrous oxide evolution from soil driven by rainfall events: 1. Model structure and sensitivity, *J. Geophys. Res.*, 97, 9759–9776, 1992.

Liang, X., Lettenmaier, D. P., Wood, E. F., and Burges, S. J.: A Simple hydrologically based model of land surface water and energy fluxes for GSMs, *J. Geophys. Res.*, 99, 415–44, 1994.

Lin, J. P.: Review of published export coefficient and event mean concentration (EMC) data, No. ERDC-TN-WRAP-04-3, Engineer Research and Development Center, Vicksburg MS, 2004.

Lohse, K. A., Brooks, P. D., McIntosh, J. C., Meixner, T., and Huxman, T. E. Interactions between biogeochemistry and hydrologic systems, *Annu. Rev. Env. Resour.*, 34, 65–96, 2009.

Mantovan, P. and Todini, E.: Hydrological forecasting uncertainty assessment: incoherence of the GLUE methodology, *J. Hydrol.*, 330, 368–381, 2006.

Mantovan, P., Todini, E., and Martina, M. L. V.: Reply to comment by Keith Beven, Paul Smith, and Jim Freer on “Hydrological forecasting uncertainty assessment: incoherence of the GLUE methodology”, *J. Hydrol.*, 338, 319–324, 2007.

Milly, P. C. D., Wetherald, R. T., Dunne, K. A., and Delworth, T. L.: Increasing risk of great floods in a changing climate, *Nature*, 415, 514–517, 2002.

McDonnell, J. J., Sivapalan, M., Vache, K., Dunn, S., Grant, G., Haggerty, R., Hinz, C., Hooper, R., Kirchner, J., Roderick, M. L., Selker, J., and Weiler, M.: Moving beyond heterogeneity and process complexity: A new vision for watershed hydrology, *Water Resour. Res.*, 43, W07301, doi:10.1029/2006WR005467, 2007.

Moriasi, D. N., Arnold, J. G., Van Liew, M. W., Binger, R. L., Harmel, R. D., and Veith, T.: Model evaluation guidelines for systematic quantification of accuracy in watershed simulations, *T. ASABE*, 50, 885–900, 2007.

HESSD

12, 4997–5053, 2015

Integrated water system simulation

Y. Y. Zhang et al.

[Title Page](#)[Abstract](#)[Introduction](#)[Conclusions](#)[References](#)[Tables](#)[Figures](#)[⏪](#)[⏩](#)[◀](#)[▶](#)[Back](#)[Close](#)[Full Screen / Esc](#)[Printer-friendly Version](#)[Interactive Discussion](#)

- Neitsch, S., Arnold, J., Kiniry, J., and Williams, J. R.: SWAT2009 Theoretical Documentation, Texas Water Resources Institute, Temple, Texas, 2011.
- Onstad, C. A. and Foster, G. R.: Erosion modeling on a watershed, *T.ASAE*, 18, 288–292, 1975.
- 5 Paola, C., Fofoula-Georgiou, E., Dietrich, W. E., Hondzo, M., Mohrig, D., Parker, G., Power, M. E., Rodriguez-Iturbe, I., Voller, V., Wilcock, P.: Toward a unified science of the Earth's surface: opportunities for synthesis among hydrology, geomorphology, geochemistry, and ecology, *Water Resour. Res.*, 42, W03S10, doi:10.1029/2005WR004336, 2006.
- Pimentel, D., Berger, B., Filiberto, D., Newton, M., Wolfe, B., Karabinakis, E., Clark, S., Poon, E., Abbett, E., and Nandagopal, S.: Water resources: agricultural and environmental issues, *Bioscience*, 54, 909–918, 2004.
- 10 Pushpalatha, R., Perrin, C., Le Moine, N., and Andréassian, V.: A review of efficiency criteria suitable for evaluating low-flow simulations, *J. Hydrol.*, 420, 171–182, 2012.
- Rallison, R. E. and Miller, N.: Past, present and future SCS runoff procedure., in: Rainfall runoff relationship, edited by: Singh, V. P., Water Resources Publication, Littleton, CO, 353–364, 1981.
- 15 Rahaman, M. M. and Varis, O.: Integrated water resources management: evolution, prospects and future challenges, *sustainability: science, Practice and Policy*, 1, 15–21, 2005.
- Revenga, C., Brunner, J., Henninger, N., Kassem, K., and Payne, R.: Pilot analysis of global ecosystems: freshwater systems, Washington DC: World Resources Institute, available at: http://pdf.wri.org/page_freshwater.pdf (20 May 2015), 2000.
- 20 Ritchie, J. T.: A model for predicting evaporation from a row crop with incomplete cover, *Water Resour. Res.*, 8, 1205–1213, 1972.
- Ritter, A. and Muñoz-Carpena, R.: Performance evaluation of hydrological models: statistical significance for reducing subjectivity in goodness-of-fit assessments, *J. Hydrol.*, 480, 33–45, 2013.
- 25 Pohlert, T., Breuer, L., Huisman, J. A., and Frede, H.-G.: Integration of a detailed biogeochemical model into SWAT for improved nitrogen predictions-model development, sensitivity and uncertainty analysis, *Ecol. Model.*, 203, 215–228, 2006.
- 30 Pohlert, T., Breuer, L., Huisman, J. A., and Frede, H.-G.: Assessing the model performance of an integrated hydrological and biogeochemical model for discharge and nitrate load predictions, *Hydrol. Earth Syst. Sci.*, 11, 997–1011, doi:10.5194/hess-11-997-2007, 2007.

Integrated water system simulation

Y. Y. Zhang et al.

[Title Page](#)[Abstract](#)[Introduction](#)[Conclusions](#)[References](#)[Tables](#)[Figures](#)[⏪](#)[⏩](#)[◀](#)[▶](#)[Back](#)[Close](#)[Full Screen / Esc](#)[Printer-friendly Version](#)[Interactive Discussion](#)

- Schiermeier, Q.: Increased flood risk linked to global warming, *Nature*, 470, 316, doi:10.1038/470316a, 2011.
- Sharples, A. N. and Williams, J. R.: EPIC-erosion/productivity impact calculator: 1. Model documentation, Technical Bulletin-United States Department of Agriculture Agric. Res. Service, Washington DC, USA, 1990.
- 5 Singh, V. P. and Woolhiser, D. A.: Mathematical modeling of watershed hydrology, *J. Hydrol. Eng.*, 7, 270–292, 2002.
- Sivapalan, M. and Kalma, J. D.: Scale problems in hydrology: contributions of the Robertson Workshop, *Hydrol. Process.*, 9, 243–250, 1995.
- 10 van Griensven, A., Meixner, T., Grunwald, S., Bishop, T., Diluzio, M., and Srinivasan, R.: A global sensitivity analysis tool for the parameters of multi-variable catchment models, *J. Hydrol.*, 324, 10–23, 2006.
- Vinogradov, Y. B., Semenova, O. M., and Vinogradova, T. A.: An approach to the scaling problem in hydrological modelling: the deterministic modelling hydrological system, *Hydrol. Process.*, 25, 1055–1073, 2011.
- 15 Vörösmarty, C. J., McIntyre, P. B., Gessner, M. O., Dudgeon, D., Prusevich, A., Green, P., Glidden, S., Bunn, S. E., Sullivan, C. A., Reidy L. C., and Davies, P. M.: Global threats to human water security and river biodiversity, *Nature*, 467, 555–561, 2010.
- Wang, G. S., Xia, J., Tan, G., and Lu, A. F.: A research on distributed time variant gain model: a case study on Chao River basin (in Chinese), *Prog. Geogr.*, 21, 573–582, 2002.
- 20 Wang, G., Xia, J., and Chen, J.: Quantification of effects of climate variations and human activities on runoff by a monthly water balance model: a case study of the Chaobai River basin in northern China. *Water Resour. Res.*, 45, W00A11, doi:10.1029/2007WR006768, 2009.
- Wang, J. Q., Ma, W. Q., Jiang, R. F., and Zhang, F. S.: Analysis about amount and ratio of basal fertilizer and topdressing fertilizer on rice, wheat, maize in China, *Chin. J. Soil Sci.*, 39, 329–333, 2008.
- 25 Wang, X.: Summary of Huaihe River Basin and Shandong Peninsula Integrated Water Resources Plan, *China Water Resour.*, 23, 112–114, 2011.
- Wigmosta, M. S., Vail, L. W., and Lettenmaier, D. P.: A distributed hydrology-vegetation model for complex terrain, *Water Resour. Res.*, 30, 1665–1679, 1994.
- 30 Wilhite, D. A.: Drought and water crises: science, technology and management issues, CRC Press, Boca Raton, FL, 2005.

HESSD

12, 4997–5053, 2015

Integrated water system simulation

Y. Y. Zhang et al.

[Title Page](#)[Abstract](#)[Introduction](#)[Conclusions](#)[References](#)[Tables](#)[Figures](#)[⏪](#)[⏩](#)[◀](#)[▶](#)[Back](#)[Close](#)[Full Screen / Esc](#)[Printer-friendly Version](#)[Interactive Discussion](#)

- Williams, J. R., Jones, C. A., and Dyke, P. T.: Modeling approach to determining the relationship between erosion and soil productivity, *Trans. ASAE*, 27, 129–144, 1984.
- Williams, J. R., Jones, C. A., Kiniry, J. R., and Spanel, D. A.: The EPIC crop growth model, *Trans. ASAE*, 32, 497–511, 1989.
- 5 Xia, J.: Identification of a constrained nonlinear hydrological system described by volterra functional series, *Water Resour. Res.*, 27, 2415–2420, 1991.
- Xia, J., Wang, G. S., Tan, G., Ye, A. Z., and Huang, G. H.: Development of distributed time-variant gain model for nonlinear hydrological systems, *Sci. China: Earth Sci.*, 48, 713–723, 2005.
- 10 Xing, G. X. and Zhu, Z. L.: An assessment of N loss from agricultural fields to the environment in China, *Nutr. Cycl. Agroecosys.*, 57, 67–73, 2000.
- Zhai, X. Y., Zhang, Y. Y., Wang, X. L., Xia, J., and Liang, T.: Non-point source pollution modeling using Soil and Water Assessment Tool and its parameter sensitivity analysis in Xin'anjiang Catchment, China, *Hydrol. Process.*, 28, 1627–1640, 2014.
- 15 Zhang, Y. Y., Xia, J., Shao, Q. X., and Zhai, X. Y.: Water quantity and quality simulation by improved SWAT in highly regulated Huai River Basin of China, *Stoch. Env. Res. Risk A.*, 27, 11–27, 2013.
- Zhou, Y., Khu, S. T., Xi, B., Su, J., Hao, F., Wu, J., and Huo, S.: Status and challenges of water pollution problems in China: learning from the European experience, *Environ. Earth Sci.*, 72, 1243–1254, 2014.
- 20 Zhu, Z. L.: Loss of fertilizer N from plants-soil system and the strategies and techniques for its reduction, *Soil Environ. Sci.*, 9, 1–6, 2000.

[Title Page](#)[Abstract](#)[Introduction](#)[Conclusions](#)[References](#)[Tables](#)[Figures](#)[|◀](#)[▶|](#)[◀](#)[▶](#)[Back](#)[Close](#)[Full Screen / Esc](#)[Printer-friendly Version](#)[Interactive Discussion](#)**Table 1.** The data sets and their categories used in the d model.

Category	Data	Objectives	Controlled processes
GIS	DEM	Elevation, slopes and lengths of each sub-basin and channel	Hydrology and water quality
	Land use map	Land use types and their corresponding areas in each subbasin	Hydrology, water quality and ecology
	Soil map	Soil physical properties of each subbasin such as bulk density, texture, saturated conductivity	
Weather	Daily precipitation	Daily precipitation of each subbasin	Hydrology
	Daily maximum and minimum temperature	Daily maximum and minimum temperature of each subbasin	
Hydrology	Runoff observations	Hydrological parameter calibration	Hydrology
Water quality	The urban wastewater discharge outlets and the discharge load	Model input of point source pollutant load	Water quality
	The concentration observation	Water quality parameter calibration	
Ecology	Crop yield, Leaf area index	Ecological parameter calibration	Ecology
Economy	The basic economic statistical indicators	Populations, breeding stock of large animals and livestock, water withdrawal in each subbasin	Hydrology and water quality
Water projects	The reservoir's design data attribute parameters	Regulation rules of reservoirs or sluices	Hydrology
Agricultural management	Fertilization types, timing and amount, the time of seeding and harvest, crop types	Agricultural management rules of each subbasin	Water quality and ecology

Integrated water
system simulation

Y. Y. Zhang et al.

Table 2. The agricultural management scheme in the Shaying River Catchment.

Crop	Management	Time		Ratio distribution of annual TN fertilizer	Ratio distribution of annual TP fertilizer	Fertilizer intensity (kg ha ⁻¹)	
		Start (month–day)	Duration (day)			TN	TP
Early rice	Base fertilization	4–1	1	0.60	0.86	40.60–86.17	25.46–59.47
	Plant	4–15	1	–	–	–	–
	Additional Fertilization	5–1	1	0.40	0.14	27.06–57.45	4.14–9.68
	Harvest and Kill	7–31	1	–	–	–	–
Late rice	Base fertilization	8–1	1	0.50	0.86	33.83–71.81	25.46–59.47
	Plant	8–15	1	–	–	–	–
	Additional Fertilization	9–1	1	0.50	0.14	33.83–71.81	4.14–9.68
	Harvest and Kill	10–31	1	–	–	–	–
Winter wheat	Base fertilization	10–1	1	0.64	0.02	43.30–271.04	0.59–4.10
	Plant	10–15	1	–	–	–	–
	Additional Fertilization	1–1	1	0.36	0.98	24.36–152.46	29.00–201.11
Cron	Harvest and Kill	6–1	1	–	–	–	–
	Base fertilization	6–1	1	0.41	0.88	27.74–173.63	26.05–180.59
	Plant	6–15	1	–	–	–	–
	Additional Fertilization	7–15	1	0.59	0.12	39.92–249.86	3.55–24.62
	Harvest and Kill	9–30	1	–	–	–	–

Title Page

Abstract

Introduction

Conclusions

References

Tables

Figures

I ◀

▶ I

◀

▶

Back

Close

Full Screen / Esc

Printer-friendly Version

Interactive Discussion



Table 3. Sensitive parameters, their value ranges and relative importance for runoff and $\text{NH}_4\text{-N}$ simulations.

Variables	Range	Definition	Relative Importance for runoff (%)	Relative Importance for $\text{NH}_4\text{-N}$ (%)
W_{fc}	0.20–0.45	Field capacity of soil	32.73	11.10
W_{sat}	0.45–0.75	Saturated moisture capacity of soil	11.68	11.83
g_1	0–3	Basic surface runoff coefficient	7.30	10.34
g_2	0–3	Influence coefficient of soil moisture	10.54	12.11
K_{ET}	0–3	Adjustment factor of evapotranspiration	23.21	10.71
K_r	0–1	Interflow yield coefficient	9.55	3.20
T_g	1–100	Delay time for aquifer recharge	1.74	–
K_g	0–1	Baseflow yield coefficient	2.91	–
K_{sat}	0–120	Steady state infiltration rate	0.33	–
R_d (COD)	0.02–3.4	COD deoxygenation rate at 20 °C	–	6.62
R_{set} (COD)	–0.36–0.36	COD settling rate at 20 °C	–	3.60
R_d (NH_4)	0.1–1	Bio-oxidation rate of $\text{NH}_4\text{-N}$ at 20 °C	–	1.97
K_{set} (NH_4)	0–100	Settling rate of $\text{NH}_4\text{-N}$ in the reservoirs	–	14.17
K_d (COD)	0.02–3.4	COD deoxygenation rate in the reservoirs at 20 °C	–	2.12
K_d (NH_4)	0.1–1.0	Bio-oxidation rate of $\text{NH}_4\text{-N}$ in the reservoirs at 20 °C	–	4.51
Total relative importance			100.00	92.27

Title Page

Abstract

Introduction

Conclusions

References

Tables

Figures

I ◀

▶ I

◀

▶

Back

Close

Full Screen / Esc

Printer-friendly Version

Interactive Discussion



Integrated water
system simulation

Y. Y. Zhang et al.

Title Page

Abstract

Introduction

Conclusions

References

Tables

Figures

I◀

▶I

◀

▶

Back

Close

Full Screen / Esc

Printer-friendly Version

Interactive Discussion

**Table 4.** Runoff simulation results for regulated and less-regulated stations.

Stations	Periods	Daily flow				Monthly flow			
		bias	r	NS	f	bias	r	NS	f
Regulated stations									
Luohe	Calibration	0.00	0.84	0.70	0.15	0.00	0.87	0.71	0.14
	Validation	-0.52	0.75	0.51	0.42	-0.52	0.87	0.67	0.33
Zhoukou	Calibration	0.24	0.87	0.73	0.21	0.24	0.90	0.76	0.19
	Validation	0.41	0.79	0.55	0.36	0.41	0.91	0.70	0.26
Huaidian	Calibration	0.03	0.88	0.77	0.13	0.03	0.91	0.81	0.10
	Validation	0.12	0.76	0.54	0.27	0.12	0.87	0.70	0.18
Fuyang	Calibration	0.00	0.90	0.81	0.10	0.00	0.95	0.89	0.05
	Validation	0.14	0.88	0.76	0.17	0.14	0.94	0.86	0.11
Yingshang	Calibration	-0.13	0.92	0.84	0.12	-0.13	0.92	0.84	0.12
	Validation	0.16	0.87	0.74	0.18	0.16	0.93	0.82	0.13
Less-regulated stations									
Shenqiu	Calibration	0.00	0.91	0.82	0.09	0.00	0.94	0.88	0.06
	Validation	-0.13	0.83	0.67	0.21	-0.13	0.98	0.94	0.08

Integrated water
system simulation

Y. Y. Zhang et al.

Table 5. The runoff simulation results at regulated stations with and without the dam regulation considered. Range means the difference of objective function value between regulations considered and not considered. If the range value is less than 0.0, then the simulation with regulation is better than that without regulation. Otherwise, the simulation without regulation is better.

Stations	Regulated capacity (%)	Flow event	Regulation considered				Regulation not considered				Range
			bias	r	NS	f	bias	r	NS	f	
Luohe	0.26	High	-0.16	0.97	0.92	0.09	-0.62	0.97	0.80	0.29	-0.20
		Low	-0.02	0.98	0.69	0.12	-1.46	0.99	-5.53	2.67	-2.55
		Average	-0.15	0.97	0.93	0.08	-0.68	0.96	0.82	0.30	-0.22
Zhoukou	1.31	High	0.21	0.98	0.93	0.10	-0.38	0.98	0.87	0.18	-0.08
		Low	1.00	0.00	-2.57	1.86	-0.64	0.99	-0.08	0.58	1.28
		Average	0.30	0.99	0.93	0.13	-0.41	0.98	0.89	0.18	-0.05
Huaidian	1.37	High	0.02	0.98	0.95	0.03	-0.64	0.98	0.68	0.32	-0.29
		Low	0.36	0.97	0.43	0.32	-1.51	0.98	-5.88	2.80	-2.48
		Average	0.06	0.98	0.96	0.04	-0.74	0.98	0.72	0.35	-0.31
Fuyang	2.21	High	0.04	0.98	0.96	0.03	-0.39	0.99	0.86	0.18	-0.15
		Low	0.17	0.99	0.87	0.10	-1.43	0.99	-3.78	2.07	-1.97
		Average	0.05	0.99	0.97	0.03	-0.50	0.99	0.88	0.21	-0.18
Yingshang	1.76	High	0.03	0.98	0.95	0.03	-0.44	0.99	0.86	0.20	-0.17
		Low	0.18	0.99	0.82	0.12	-1.77	0.95	-9.26	4.03	-3.91
		Average	0.05	0.99	0.96	0.03	-0.60	0.98	0.86	0.25	-0.22

Title Page

Abstract

Introduction

Conclusions

References

Tables

Figures

I◀

▶I

◀

▶

Back

Close

Full Screen / Esc

Printer-friendly Version

Interactive Discussion



Table 6. The comparison of $\text{NH}_4\text{-N}$ simulation results between with and without dam regulation considered.

Stations	Periods	Regulated			Unregulated			Range	Ratio of non-point source load (%)
		bias	r	f	bias	r	f		
Regulated stations									
Luohe	Calibration	-0.02	0.93	0.05	-0.67	0.60	0.54	-0.49	46.10
	Validation	-	-	-	-	-	-	-	-
Zhoukou	Calibration	0.29	0.61	0.34	-0.56	0.38	0.59	-0.25	44.54
	Validation	0.27	0.56	0.36	-1.35	0.66	0.85	-0.49	-
Huaidian	Calibration	0.22	0.73	0.25	0.49	0.80	0.35	-0.10	31.72
	Validation	0.02	0.67	0.18	0.22	0.51	0.36	-0.18	-
Fuyang	Calibration	0.28	0.78	0.25	0.26	0.80	0.23	0.02	33.12
	Validation	-0.27	0.76	0.26	-0.38	0.56	0.41	-0.15	-
Yingshang	Calibration	0.24	0.79	0.23	0.25	0.58	0.34	-0.11	33.26
	Validation	-0.24	0.49	0.38	-0.76	0.62	0.57	-0.19	-
Less-regulated stations									
Shenqiu	Calibration	0.13	0.62	0.26	-	-	-	-	47.13
	Validation	0.16	0.41	0.37	-	-	-	-	-

Title Page

Abstract

Introduction

Conclusions

References

Tables

Figures

I ◀

▶ I

◀

▶

Back

Close

Full Screen / Esc

Printer-friendly Version

Interactive Discussion



HESSD

12, 4997–5053, 2015

Integrated water system simulation

Y. Y. Zhang et al.

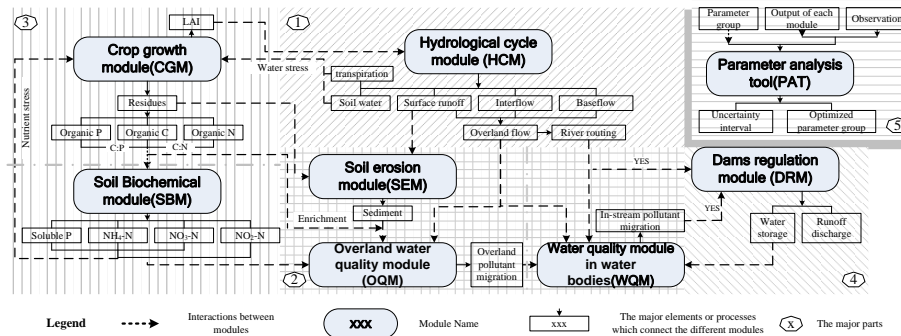


Figure 1. The model structure and the interactions among the major modules (1: hydrological part; 2: water quality part; 3: ecological part; 4: dam regulation part; 5: parameter analysis tool).

Title Page	
Abstract	Introduction
Conclusions	References
Tables	Figures
⏪	⏩
⏴	⏵
Back	Close
Full Screen / Esc	
Printer-friendly Version	
Interactive Discussion	



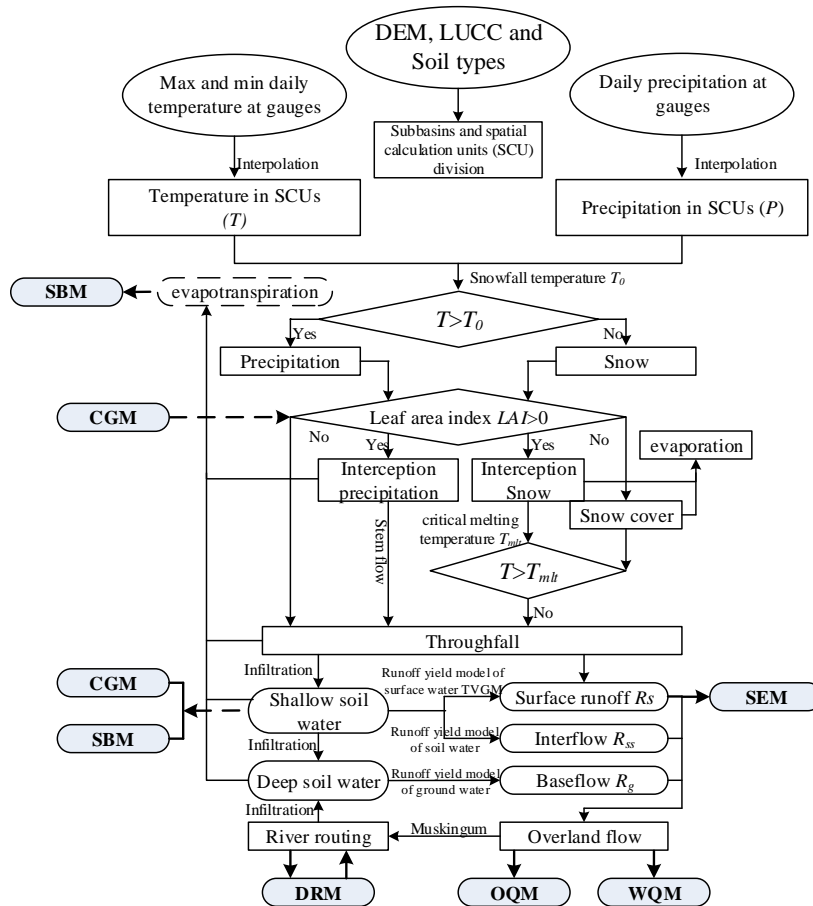


Figure 2. The flowchart of hydrological cycle module and the interactions with other modules.

Title Page

Abstract Introduction

Conclusions References

Tables Figures

◀ ▶

◀ ▶

Back Close

Full Screen / Esc

Printer-friendly Version

Interactive Discussion



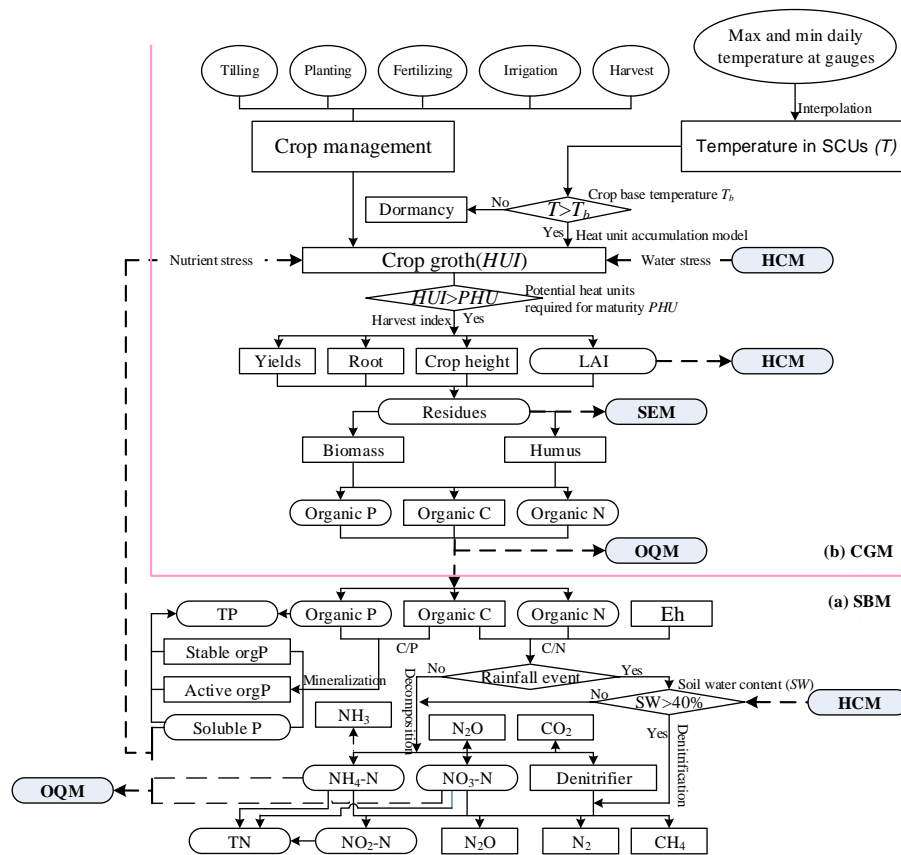


Figure 3. The flowchart of soil biochemical module (a) and crop growth module (b) in ecological part and the interactions with other modules.

Integrated water system simulation

Y. Y. Zhang et al.

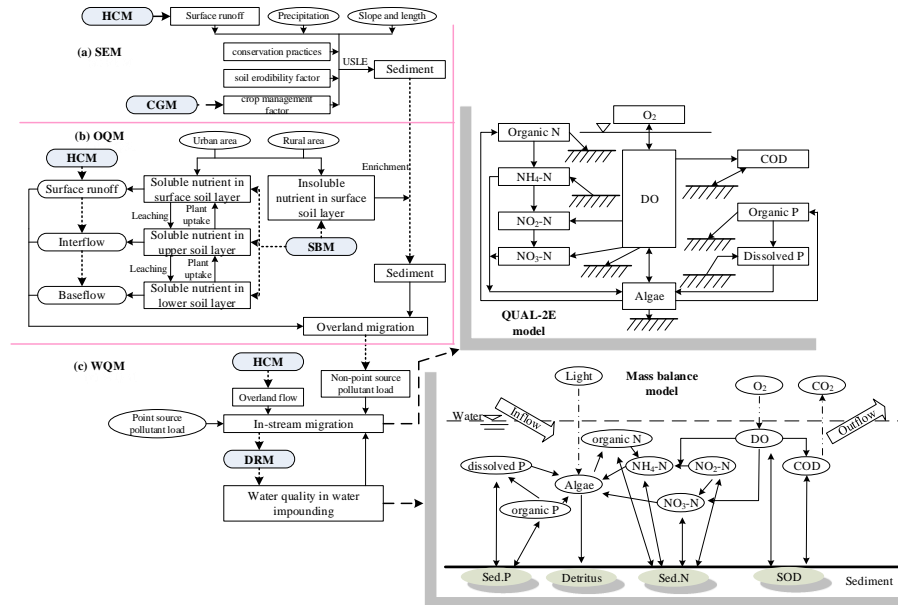


Figure 4. The flowchart of soil erosion module (a), overland water quality module (b) and water quality module of water bodies (c) in water quality part and the interactions with other modules.

Title Page	
Abstract	Introduction
Conclusions	References
Tables	Figures
◀	▶
◀	▶
Back	Close
Full Screen / Esc	
Printer-friendly Version	
Interactive Discussion	



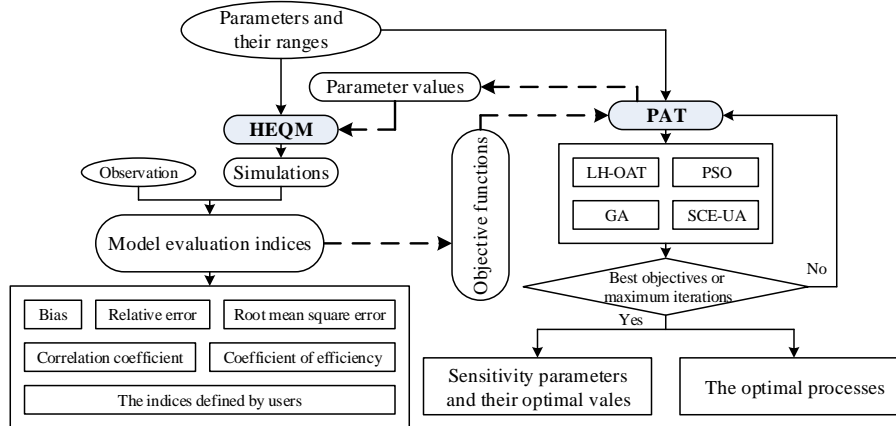


Figure 5. The flowchart of parameter analysis tool and the interactions with the developed model.

Title Page

Abstract	Introduction
Conclusions	References
Tables	Figures

⏪
⏩

◀
▶

Back
Close

Full Screen / Esc

Printer-friendly Version

Interactive Discussion



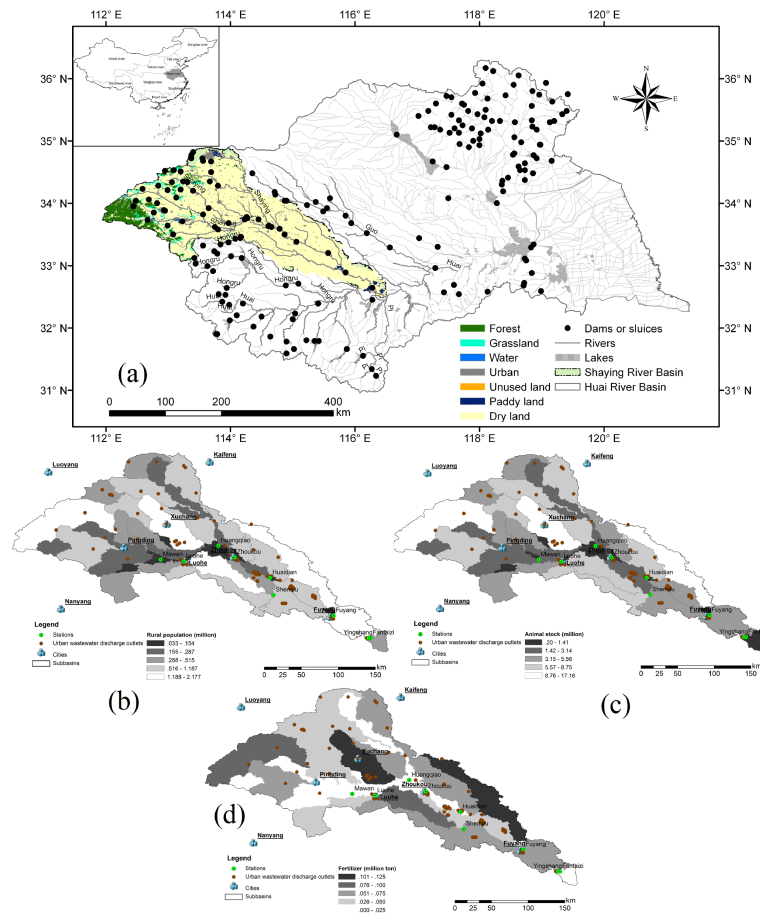


Figure 6. The location of study area (a) and the digital delineation of subbasin, point source pollutant outlets, rural population (b), animal stock (c) and fertilization (d).

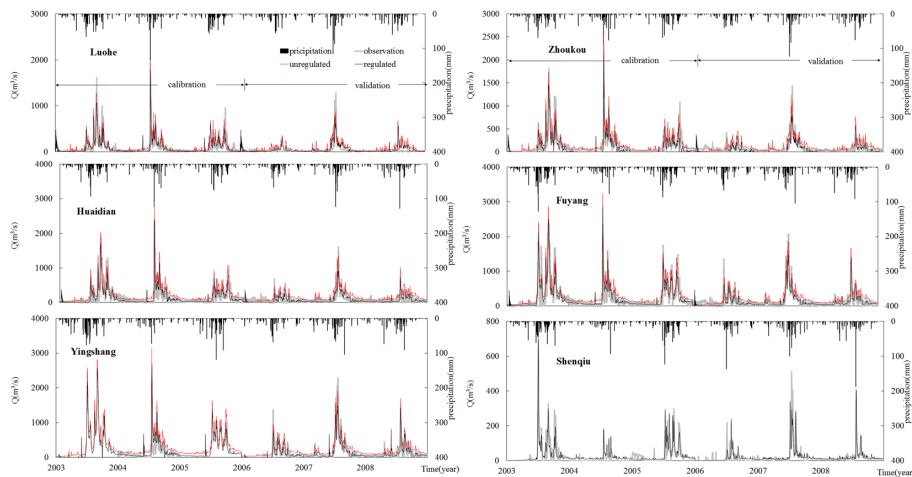


Figure 7. The daily runoff simulation at all the stations.

[Title Page](#)
[Abstract](#)
[Introduction](#)
[Conclusions](#)
[References](#)
[Tables](#)
[Figures](#)
[◀](#)
[▶](#)
[◀](#)
[▶](#)
[Back](#)
[Close](#)
[Full Screen / Esc](#)
[Printer-friendly Version](#)
[Interactive Discussion](#)

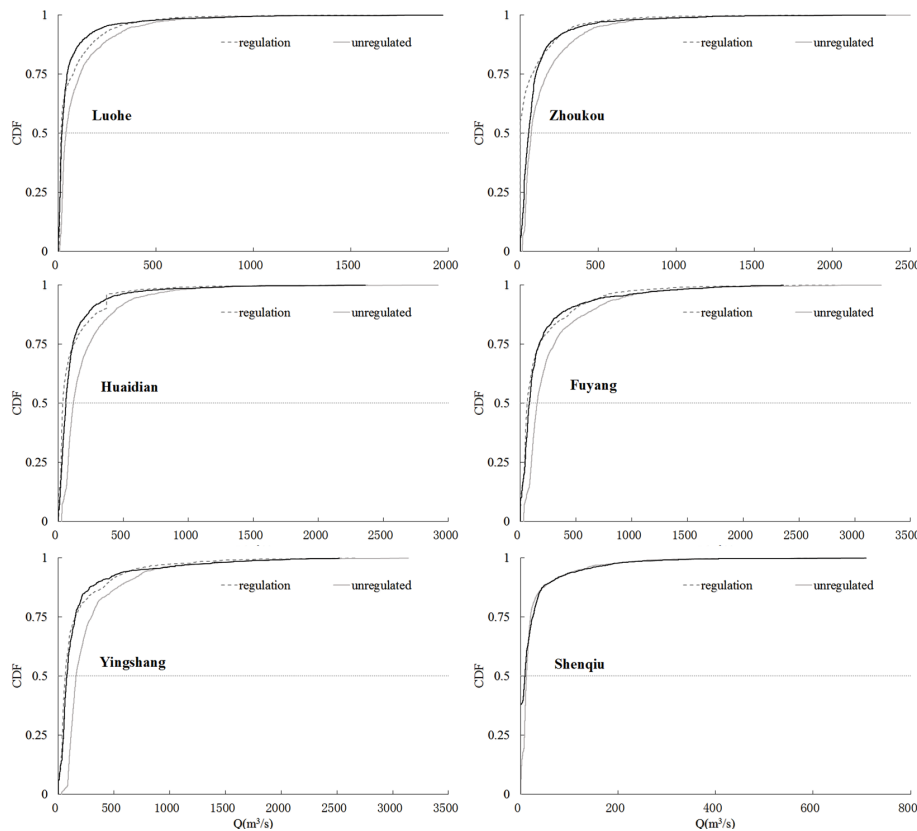



Figure 8. The cumulative distributions of simulated and observed daily runoff at all the stations.

[Title Page](#)[Abstract](#)[Introduction](#)[Conclusions](#)[References](#)[Tables](#)[Figures](#)[⏪](#)[⏩](#)[◀](#)[▶](#)[Back](#)[Close](#)[Full Screen / Esc](#)[Printer-friendly Version](#)[Interactive Discussion](#)

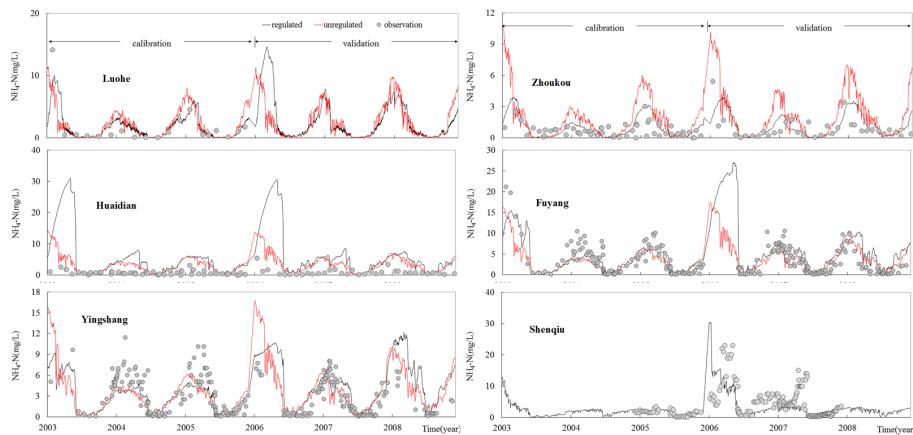


Figure 9. The simulated $\text{NH}_4\text{-N}$ concentration variation at all the situations.

[Title Page](#)
[Abstract](#)
[Introduction](#)
[Conclusions](#)
[References](#)
[Tables](#)
[Figures](#)
[⏪](#)
[⏩](#)
[⏴](#)
[⏵](#)
[Back](#)
[Close](#)
[Full Screen / Esc](#)
[Printer-friendly Version](#)
[Interactive Discussion](#)

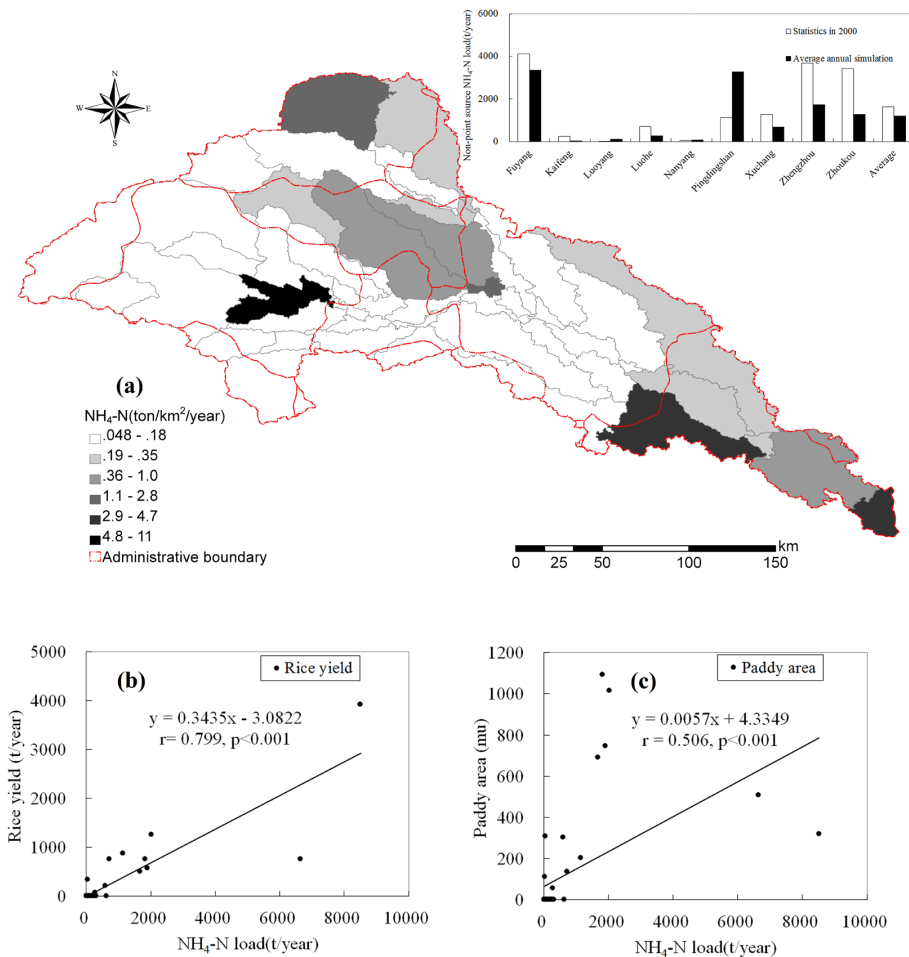



Figure 10. The spatial pattern of nonpoint source $\text{NH}_4\text{-N}$ load **(a)** and its relationship with paddy area **(b)** and rice yield **(c)** at the subbasin and regional scale in the Shaying River Catchment.

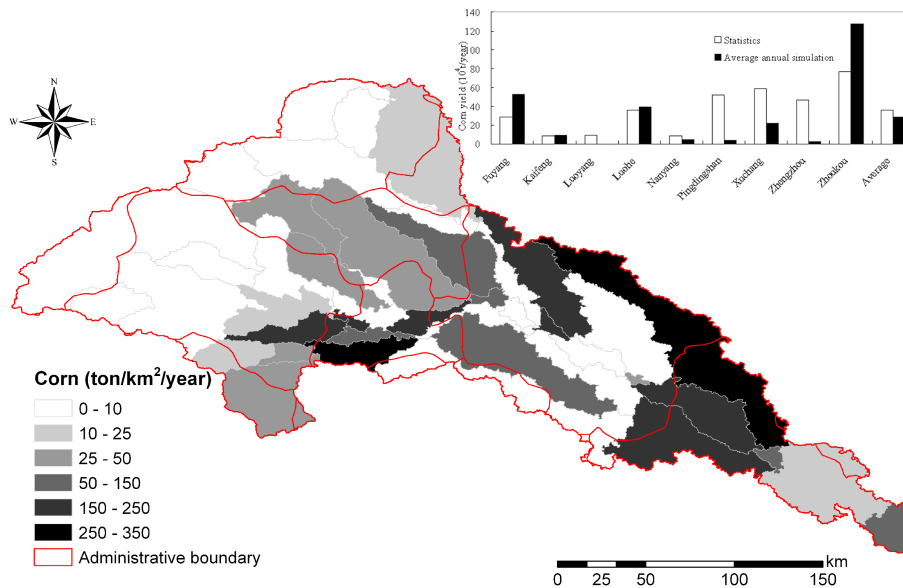


Figure 11. The spatial pattern of corn yield at the subbasin and regional scale in the Shaying River Catchment.